



HAL
open science

Variability of effects of spatial climate data aggregation on regional yield simulation by crop models

Holger Hoffmann, Gang Zhao, Lenny G. J. van Bussel, Andreas Enders, Xenia Specka, Carmen Sosa, Jagadeesh Yeluripati, Fulu Tao, Julie J. Constantin, Helene H. Raynal, et al.

► To cite this version:

Holger Hoffmann, Gang Zhao, Lenny G. J. van Bussel, Andreas Enders, Xenia Specka, et al.. Variability of effects of spatial climate data aggregation on regional yield simulation by crop models. *Climate Research*, 2015, 65, pp.53-69. 10.3354/cr01326 . hal-02636784

HAL Id: hal-02636784

<https://hal.inrae.fr/hal-02636784v1>

Submitted on 30 Sep 2024

HAL is a multi-disciplinary open access archive for the deposit and dissemination of scientific research documents, whether they are published or not. The documents may come from teaching and research institutions in France or abroad, or from public or private research centers.

L'archive ouverte pluridisciplinaire **HAL**, est destinée au dépôt et à la diffusion de documents scientifiques de niveau recherche, publiés ou non, émanant des établissements d'enseignement et de recherche français ou étrangers, des laboratoires publics ou privés.

1 **Title: Variability of spatial aggregation effects of climate data on regional yield**
2 **simulation by crop models for a selected region in Germany**

3 **Suggested running page head: Crop model climate input data aggregation effects**
4

5 *Hoffmann, Holger¹; Zhao, Gang^{1*}; van Bussel, Lenny G.J.^{1,2}; Enders, Andreas¹; Specka, Xenia³; Sosa,*
6 *Carmen⁴; Yeluripati, Jagadeesh^{5, 17}; Tao, Fulu⁶; Constantin, Julie⁷; Raynal, Helene⁷; Teixeira, Edmar⁸;*
7 *Grosz, Balázs⁹; Doro, Luca¹⁰; Zhao, Zhigan¹¹; Wang, Enli¹¹; Nendel, Claas³; Kersebaum, Kurt-Christian³;*
8 *Haas, Edwin¹²; Kiese, Ralf¹²; Klatt, Steffen¹²; Eckersten, Henrik¹³; Vanuytrecht, Eline¹⁴; Kuhnert, Matthias⁵;*
9 *Lewan, Elisabet⁴; Rötter, Reimund⁶; Roggero, Pier Paolo¹⁰; Wallach, Daniel⁷; Cammarano, Davide¹⁶,*
10 *Asseng, Senthold¹⁶; Krauss, Gunther¹; Siebert, Stefan¹; Gaiser, Thomas¹; Ewert, Frank¹*

11 ¹ Crop Science Group, Institute of Crop Science and Resource Conservation (INRES), University of Bonn, Katzenburgweg 5, 53115 Bonn, DE

12 ² Plant Production Systems Group, Wageningen University, P.O. Box 430, 6700 AK, Wageningen, NL

13 ³ Institute of Landscape Systems Analysis, Leibniz Centre for Agricultural Landscape Research, 15374 Müncheberg, DE

14 ⁴ Biogeophysics and water quality, Department of Soil and Environment, Swedish University of Agricultural Sciences, Lennart Hjelms väg 9, 750
15 07 Uppsala, SE

16 ⁵ Institute of Biological and Environmental Sciences, School of Biological Sciences, University of Aberdeen, 23 St Machar Drive, Aberdeen AB24
17 3 UU, Scotland, UK

18 ⁶ Climate Impacts Group, Natural Resources Institute Finland (Luke), 00790 Helsinki, FI

19 ⁷ INRA, UMR 1248 AGIR & UR0875 MIA-T, F-31326 Auzeville, FR

20 ⁸ Systems Modelling Team (Sustainable Production Group), The New Zealand Institute for Plant and Food Research Limited, Canterbury
21 Agriculture & Science Centre, Gerald St, Lincoln 7608, NZ

22 ⁹ Thünen-Institute of Climate-Smart-Agriculture, Bundesallee 50, 38116 Braunschweig, DE

23 ¹⁰ Desertification Research Group, Università degli Studi di Sassari, Viale Italia 39, 07100 Sassari, IT

24 ¹¹ CSIRO Land and Water, Clunies Ross Street, Canberra, ACT, AU

25 ¹² Institute of Meteorology and Climate Research – Atmospheric Environmental Research, Karlsruhe Institute of Technology,
26 Kreuzeckbahnstraße 19, 82467 Garmisch-Partenkirchen, DE

27 ¹³ Department of Crop Production Ecology, Swedish University of Agricultural Sciences, Ulls väg 16, 750 07 Uppsala, SE

28 ¹⁴ Division Soil & Water Management, KU Leuven, Celestijnenlaan 200E, PO 2411, 3001 Heverlee, BE

29 ¹⁶ Agricultural & Biological Engineering Department, University of Florida, Frazier Rogers Hall, Gainesville, FL 32611, USA

30 ¹⁷ The James Hutton Institute, Craigiebuckler, Aberdeen AB15 8QH, UK

31 *Corresponding author: Holger Hoffmann, Tel: (+49) 228 73 2876, fax: (+49) 228 73 2870, email: hhoffmann@uni-
32 bonn.de

33 **Abstract** Field-scale crop models are often applied at coarser spatial resolutions than the field.
34 However, little is known on the response of the models to spatially aggregated climate input data
35 and why these responses can differ across models. Depending on the model, regional yield estimates
36 from large-scale simulations may therefore be biased as compared to simulations with high-
37 resolution input data.

38 We therefore evaluated this so-called aggregation effect for 13 crop models for a selected region in
39 Germany. For this purpose, the models were supplied with climate data of 1 km resolution and
40 spatial aggregates of up to 100 km resolution raster. The models were used with two crops (winter
41 wheat and silage maize) and three production situations (potential, water limited and nitrogen-
42 water-limited growth) to improve the understanding of errors in model simulations related to data
43 aggregation and possible interactions with the model structure. The most important climate
44 variables identified to determining the model-specific input data aggregation on simulated yields
45 were mainly related to changes in radiation (winter wheat) and temperature (silage maize).
46 Additionally, aggregation effects were systematic since models differed in the systematic fraction of
47 the aggregation effect, regardless of the extent of the effect (20 to 66 % as compared to 1.7 % for
48 random effects). Climate input data aggregation changed the mean simulated regional yield up to
49 0.2 t ha^{-1} , whereas simulated yields from single years and models differed considerably depending
50 on the data aggregation. This implies that large-scale crop yield simulations are robust against
51 climate data aggregation on average. However, they can be systematically biased at higher temporal
52 or spatial resolutions, depending on the model and its parametrization.

53

54 **Key words:** Spatial aggregation effects, climate, crop simulation model, input data, scaling,
55 variability, yield simulation, model comparison

56 **1) Introduction**

57 Process-based crop models have typically been developed for the field-scale, for which model
58 driving variables (e.g. soil variables) are easily obtained (Van Ittersum et al. 2003, Hansen et al.
59 2006). However, crop models are increasingly used for large-scale simulations (Chipanshi et al. 1998,
60 Folberth et al. 2012). Scale in the following refers to the spatial extent and resolution of a given grid
61 cell size, ignoring temporal scales (van Bussel et al. 2011a, Weihermüller et al. 2011). Thus, using
62 field-scale crop models with input data at scales other than they were developed for, raises the
63 question how the choice of scale influences the simulation outputs. Changing the spatial resolution
64 by aggregation or disaggregation of data bears the risk of missing the relevant scale of a process or
65 phenomenon, since these are often scale dependent (Meentemeyer 1989). Thus, it is essential to
66 determine the impact of input data (dis-)aggregation on crop model outputs.

67 Although the relevance of scale (Hansen & Jones 2000, Ewert et al. 2011, Nendel et al., 2013) and
68 spatial data aggregation (Gardner et al. 1982, Cale et al. 1983, Cale & O'Neill 1988, Rastetter et al.
69 1992, Pierce & Running 1995, Nungesser et al. 1999, Gong et al. 2003, Syphard & Franklin 2004,
70 Lorite IJ et al. 2005, Ershadi et al. 2013) are well-known and data aggregation has been addressed for
71 instance in soil or hydrological process modelling (Heuvelink & Pebesma 1999, Haverkamp et al.
72 2005, Leopold et al. 2006, Bormann et al. 2009), few studies have characterized the impact in
73 application of crop models with spatially aggregated climate input data on simulated regional yields,
74 hereinafter called aggregation effect. For instance, De Wit et al. (2005) used precipitation and
75 radiation aggregated from 10 km to 50 km resolution as model input to simulate winter wheat and
76 grain maize yields in Germany and France. These yields showed a root mean square error (RMSE) of
77 0.33 t ha^{-1} ($R^2 > 0.96$) and a low bias between results from 10 and 50 km resolutions (estimated from
78 Fig. 4, De Wit et al. 2005). This low bias is in agreement with findings of Folberth et al. (2012) who
79 found small differences in maize yields in the U.S. within resolutions of 7.5 to 45 km resolution. Also
80 Angulo et al. (2013) found small differences in spring barley yields in Finland within resolutions of 10

81 to 100 km. Similarly, Van Bussel et al. (2011) reported a low bias in simulated winter wheat
82 phenology using aggregated temperatures and sowing dates. Thus, aggregation of climate input data
83 at resolutions of 10 to 100 km could be expected to have low impact on crop model output. This
84 should be considered for instance in large-scale simulations, since data aggregation may destroy
85 physical consistency (Hoffmann & Rath 2012) or combine data beyond the meaningful range of the
86 underlying process. The latter may be taken into account by keeping aggregated grid size below the
87 range estimated via semivariogram models (Brown et al. 1992, Artan et al. 2000). While this previous
88 research indicates the spatial resolution at which crop models may be applied without larger errors
89 in the average simulated crop yields, this research only represented a small sample of crop models
90 and output variables. Furthermore, the systematic behaviour of aggregation effects of models across
91 scales, production situations or crops has not been quantified beyond reporting magnitude and
92 distribution.

93 We hypothesize that crop models differ in their sensitivity to climate input data aggregation as well
94 as in the fraction of explained variance of the aggregation effects. It is however unknown, whether
95 this affects regional yield estimates from simulations in a systematic way. The objective of this work
96 is therefore to compare the response of regional yields simulated by crop models to climate input
97 data aggregation and to propose a measure for the systematic proportion of the aggregation effects.
98

99 **2) Methods**

100 **2.1) General procedure and regional focus**

101 The hypotheses given above were tested in the state of North-Rhine Westphalia (NRW), one of the
102 larger a federal states of Germany with a total area of 34,098 km² (Cologne district council 2013).
103 NRW is characterized by a humid, temperate climate and heterogeneous topography with elevations
104 between 9 m and 843 m above sea level resulting in several agro-ecological zones with different
105 temperature and rainfall regimes. In order to assess spatial aggregation effects, climate input data
106 were aggregated to spatial resolutions varying between 1 km and 100 km (Fig. 1) and used for
107 driving crop models for simulations of winter wheat (*Triticum aestivum* L.) and silage maize (*Zea*
108 *mays* L.) for the entire state area (Fig. 2). Aggregation effects were estimated by relating model
109 output variables to varying climate inputs. Finally, main determinants of these aggregation effects
110 were identified by analyzing the relative contributions from the climate variables and separately the
111 relative importance of model variables employing Partial Least Squares Regression (PLS).

112 **2.2) Climate data processing, aggregation and characterization**

113 **Climate data.** Time series of daily minimum, mean and maximum air temperature (2 m above
114 ground), precipitation, global radiation, wind speed and relative humidity for the period 1982 to
115 2011 from 280 daily weather stations, as well as an interpolated grid of 1 km resolution of monthly
116 time series were obtained from the German Meteorological Service (DWD). The monthly grids were
117 combined with the daily weather station data as described by Zhao et al. (2014b). Regional climate
118 properties for the different resolutions are given by Table 1 and for 1 km also given by Van Bussel et
119 al. (2014).

120
121 **Grids / Aggregation.** Daily climate data in spatial resolution α of 1 km² were spatially averaged for
122 four different coarser grid sizes of 10, 25, 50 and 100 km (see the Appendix for equations). Coarser
123 grids were technically set-up starting in the north-west corner of the study region.
124

125 **Semivariance.** In order to avoid the aggregation of spatially incoherent data, the climate was
126 characterized by semivariograms, which provide information about the extent of spatial dependency
127 (Brown et al. 1993). This so-called range was estimated by fitting Gaussian (precipitation,
128 temperature) and exponential (global radiation) variogram models to the empirical semivariance
129 (Minsasny 2005, Wackernagel 1995, Webster 2001).

130

131 **Sub-regions.** Due to incomplete data coverage beyond NRW, data means of grid cells of resolutions
132 larger than 1 km and thus crossing the boundary of the state may be biased, depending on the grid
133 cell size and data coverage (Fig. S3). Therefore, all calculations were validated with the help of sub-
134 regions, being two cells of 100 km resolution and a spatial data coverage of >80 % (C0:R4 and C1:R3,
135 Fig.1) and five cells of 50 km resolution with a corresponding coverage of 100 % (z50, Fig.1).

136

137 **2.3) Crop Simulations**

138 In our study 13 models currently used in addressing different research questions at various scales
139 were selected (appendix Table 5, Suppl. 2). This model ensemble was used to simulate development,
140 growth and yield for the period 1982 to 2011 for each grid cell at each spatial resolutions for winter
141 wheat and silage maize. If not further specified in the following, yield of winter wheat refers to grain
142 yield whereas silage maize yield is aboveground biomass. Simulations (see appendix Table 6 for an
143 overview) were conducted, and both crops were evaluated for i) potential, ii) water-limited and iii)
144 nitrogen-water-limited production situations; correspondingly limited by i) temperature and
145 radiation, ii) precipitation, temperature and radiation, and iii) nitrogen, precipitation, temperature
146 and radiation (Evans and Fisher 1999; Van Ittersum and Rabbinge 1997). Models were set up with a
147 single soil profile (sandy loam; Table S1) which represents a typical deep cropland soil with high
148 water holding capacity and with a common management for any of the grid cells (Appendix Table 7).
149 Models were calibrated at 1 km resolution, using one typical sowing and one typical harvest date per
150 crop as well as the whole region weighted average winter wheat yield and aboveground biomass of
151 silage maize derived from county statistics respectively from 1999 to 2011 and from 2000 to 2008
152 (Statistische Ämter des Bundes und der Länder 2013). The county statistics are point data and
153 partially based on expert knowledge and are therefore shown only with the purpose to put results
154 into context.

155 **2.4) Model intercomparison / Taylor diagrams**

156 Crop model results were compared via Taylor diagrams (Taylor 2001), presenting the correlation
157 coefficient R , centered root-mean-square difference ($RMSD$) and standard deviations σ of all grid
158 cells and years as compared to the model ensemble mean (see the appendix for equations). R and
159 $RMSD$ show correlation and difference, respectively, of each model to the model ensemble mean.
160 SD is shown for each model as well as for the ensemble mean. Statistics were calculated from all grid
161 cells of the 1 km resolution and years, thus showing the model agreement in time and space.

162 **2.5) Probability density functions (PDFs)**

163 PDFs were obtained by kernel density estimation with a Gaussian kernel (see Hoffmann & Rath 2013
164 for equations). In order to assure comparability between the PDF of a given crop, the bandwidth was
165 kept constant to 0.1 t ha^{-1} (winter wheat) and 0.3 t ha^{-1} (silage maize).

166 **2.6) Analysis of aggregation effects**

167 **Mean regional effects.** Climate data aggregation effects were evaluated in the climate data itself
168 and in model outputs. For this purpose, regional means and spatial variances of daily climate data

169 and of annual crop model outputs were calculated as absolute differences from coarser resolutions
170 to the 1 km resolution (see appendix 8.2 for equations). Model outputs were thus analyzed only at
171 the resolution of the input data (e.g. to calculate the spatial variance) as well as the mean of the
172 entire region (e.g. to calculate regional yields).

173

174 **Fraction of directed effects.** We tested if winter wheat and silage maize yields follow a specific
175 ascending or descending order related to the order of the spatial resolution, for instance if yields at
176 100 km resolution were larger than yields at 50 km resolution and if yields at 50 km resolution were
177 larger than yields at 25 km resolution and so on. For this purpose, the fraction P of simulated yields
178 following monotonously the order or inverse order of the spatial resolutions for each model was
179 calculated (see appendix 8.2 for equations).

180

181 **Partial Least Squares Regression (PLS).** While P gives insights into the direction and behavior of
182 aggregation effects, the relevance of factors (e.g. of single climate variables) to aggregation effects
183 remains unclear. However, while the estimated effects and possible causes will be highly auto-
184 correlated, regression algorithms may fail to establish statistical relations between independent
185 (aggregated input dataset) and dependent (crop model output, e.g. yield) data (Luedeling & Gassner
186 2012). Additionally, the algorithm must handle a large number of independent variables, while
187 avoiding over fitting. In order to evaluate aggregation effects, which are likely driven by numerous
188 complementary as well as contrary processes of crop model and input data interaction, Partial Least
189 Squares Regression (PLS; also known as Projection to Latent Structures Regression) is applied. PLS
190 has been employed for similar purposes related to impacts of climate variation, i.e. on tree
191 phenology (Luedeling & Gassner 2012, Guo et al. 2013). The method takes the dependent variable
192 into account, selecting only the most relevant linear combinations for regression. We thus introduce
193 PLS as a method for quantifying the fraction of variance of aggregation effects explained by climate
194 data or model outputs. PLS was used to assess the relative importance of the climate variables and a
195 limited number of model variables to the aggregation effects.

196 Dependent variables were changes in mean yields (winter wheat) and final aboveground biomass
197 (silage maize), whereas i) the climate variables during the entire growing period, from sowing to
198 anthesis and from anthesis to maturity, as well as ii) model outputs (winter wheat grain yield, silage
199 maize aboveground biomass, maximum leaf area index, cumulative evapotranspiration, cumulative
200 intercepted photosynthetic active radiation, duration of phenological phases) were used as
201 independent variables. The importance of these variables to the aggregation effect was estimated
202 calculating the variable importance (VIP) from the PLS loadings (Wold 1994, 2001). The highest five
203 predictors with a VIP above 1 were selected.

204 (Figure 1)

205 (Figure 2)

206 **3) Results**

207 **3.1) Characterization of the climate input data: Semivariance and aggregation effects**

208 Spatial aggregation of climate time series removed climate extremes of the region, while area means
209 were stable across resolutions (Fig. 3). Consistently, the corresponding spatial variance of the
210 climate variables decreased with increasing spatial resolution. The climate variables daily mean
211 temperature, global radiation and precipitation exhibit a spatial autocorrelation in the range and
212 above the largest aggregation used in this study (Fig. 4, effective range of 93.9, 122.5 and 161.9 km
213 for precipitation, daily mean temperature and global radiation, respectively; R^2 : 0.998, 0.997, 0.995,
214 respectively). Aggregating the climate data decreases the semivariance, as shown for precipitation
215 (Fig. 4).

216 **3.2) Characterization of simulated crop yields**

217 **Crop-specific yields.** The ensemble means of simulated winter wheat and silage maize yields of the
218 region were in the range of 7.6 to 8.7 t ha⁻¹ and 15.4 to 17.6 t ha⁻¹, respectively depending on the
219 production condition (Table 2, Fig. 5). On average, simulated yields were above the observed yields
220 of 7.2 t ha⁻¹ and 14.3 t ha⁻¹, respectively.

221

222 **Temporal variability of simulated crop yields.** On average, crop models reproduced the year-to-year
223 variability of simulated yields calculated from county statistics (Fig. 5). However, the majority of the
224 models simulated a larger year-to-year variability in yields than observed. Generally, simulated
225 temporal variations of yields were better for winter wheat than for silage maize. Single year yield
226 distributions are shown exemplarily in Fig. S2.

227

228 **Influence of the production situation on simulated crop yields.** Yields decreased consistently from
229 potential to water-limited to nitrogen-water-limited production (Table 2, Fig. 5). While on average
230 water-limited winter wheat and silage maize yields were respectively 0.4 t ha⁻¹ and 1.2 t ha⁻¹ lower than
231 potential yields, they were additionally 0.6 t ha⁻¹ and 0.7 t ha⁻¹ lower under nitrogen-water-limited
232 conditions as under water-limited conditions (Table 2). Noticeably, while nitrogen availability was
233 thus limiting yields comparably stronger on average than water limitations, the latter were
234 noticeably stronger in 1996, 2010 and 2011, corresponding to 74 % of the decline in these years as
235 compared to potential conditions.

236

237 **Spatial variability of simulated crop yields.** The interquartile range of yields across the region and
238 from all three production situations was in the range (silage maize) and partially above the range
239 (winter wheat) of observations (not shown). The corresponding coefficient of variation of crop yield
240 across the region for the mean of years was up to 8.2 % and 12.9 % for winter wheat and silage
241 maize, respectively. Distributions of simulated yields across the region at 1 km resolution
242 consistently showed a negative skew in the mean (Fig. 6).

243

244 **Crop model variability in simulating yields.** Simulated yields differed across models and crops,
245 showing a higher agreement among models for winter wheat than for silage maize (Fig. 7). For
246 winter wheat, most models – with the exception of DailyDayCent and LandscapeDNDC – had a
247 standard deviation across all years and grid cells in the range of 1 t ha⁻¹, while the standard deviation
248 of the ensemble mean was about 0.5 t ha⁻¹. Similar results were found for silage maize, where
249 models showed a larger spread in the standard deviation (approximate range 1.3 to 3.5 t ha⁻¹)
250 compared to the ensemble mean (1.0 to 1.4 t ha⁻¹). However, models are more dispersed for

251 potential silage maize aboveground biomass than for potential winter wheat grain yield, with only
252 Simplace<LINTUL5> exhibiting a larger spatio-temporal standard deviation of biomass than other
253 models. Contrastingly, while simulations for winter wheat varied little between production
254 situations, simulations for silage maize showed an increasing standard deviation and *RMSD* between
255 single models and the ensemble mean of model outputs, from potential to water-limited and
256 nitrogen-water-limited production. However, correlation coefficients revealed a range of agreement
257 of 0 to 0.75 and -0.5 to 0.95 for winter wheat and silage maize, respectively, underpinning the larger
258 agreement between single models and model ensemble for wheat than for maize.

259

260 **3.3) General characterization of aggregation effects**

261 **Crop-specific aggregation effects.** Yield and biomass distributions were distinctly different for the
262 two crops and affected by aggregation (Table 2, Fig. 6). On average, aggregation of climate input
263 data led to an increase of winter wheat grain yields (Fig. 8). Mean aggregation effects up to 0.2 t ha^{-1}
264 were found for both winter wheat and silage maize, thus resulting in a lower relative aggregation
265 effect in relation to the yield for silage maize as compared to winter wheat (Table 2). While the
266 mean and maximum likelihood of yield probability density functions (PDFs) of the ensemble results
267 over the region were hardly affected by aggregation, the width was reduced with increasing
268 aggregation (Fig. 6). Contrary to the net aggregation effect of the region, crops differed in their PDF
269 as aggregation led to a mode at higher yields of winter wheat in contrast to the PDF mode of silage
270 maize.

271

272 **Temporal variability of yield aggregation effects.** Single-year aggregation effects followed no clear
273 pattern, as positive and negative aggregation effects were simulated. In some years, the aggregation
274 effect consistently increased or decreased with the resolution (see example in Fig. S2). For instance,
275 the annual mean yield of winter wheat and silage maize of the region followed the order of the
276 spatial resolutions *P* in 50.1 % and 34.9 % of all years in the mean of models, respectively.

277

278 **Spatial variability of yield aggregation effects.** With coarser spatial resolutions, grid cells located at
279 the region boundary were increasingly less represented by data (Fig. 1, Fig. S1, Fig. S3). As the
280 number of grid cells decreases with coarser spatial resolution, a higher fraction of grid cells extends
281 beyond the boundary of the region. However, analysing sub-regions of 50 and 100 km resolution,
282 revealed similar patterns for mean aggregation effects compared to the entire region of NRW (Fig.
283 8). Similar to the mean aggregation effects, extremes of aggregation effects of sub-regions were
284 comparable to those of NRW. For silage maize, however, sub-region C0:R4 showed larger
285 aggregation effects under water-limited conditions, resulting from simulations of the AquaCrop 4.0
286 model.

287

288 **Influence of the production situation on yield aggregation effects.** Aggregation effects were similar
289 in the median for all three production situations (Fig. 8), showing a similar pattern across
290 resolutions. Again, larger aggregation effects were found under water-limited conditions for silage
291 maize.

292

293 **3.4) Model-specific interaction with aggregation effects as influenced by treatments**

294

295 **Aggregation effect - crop model interaction with crop.** While aggregation effects were similar
296 among the crops for the ensemble mean, they differed largely in their extent between models (Fig.
297 8, Tables 3 and 4). The range of effects was larger on average for silage maize than for winter wheat.

298 However, some single models showed larger positive aggregation effects for silage maize (e.g.
299 HERMES), comparable aggregation effects for both crops (e.g. MONICA) or lower net aggregation
300 effects for silage maize (e.g. SIMPLACE<LINTUL5>).

301

302 **Aggregation effect - crop model interaction with time.** Crop models differed substantially in their
303 sensitivity to climate input data aggregation when single years are considered (Tables 3 and 4). Years
304 with lowest and largest aggregation effects (Fig. S4) differed among crop models with no clear
305 pattern. In addition, models differed in their fraction of yields following clearly the order of the
306 resolutions, *P*, with models ranging from 20.0 % (EPIC) to 66.1 % (HERMES). As compared to 1.7 %
307 probability for a randomly ascending or descending sequence out of 120 permutations, the results
308 indicate systematic processes. Ranking models from high to low systematic effects for winter wheat
309 yields according to *P* results in the following order: STICS > APSIM(modified) > APSIM >
310 SIMPLACE<LINTUL5> > LandscapeDNDC > HERMES > APSIM-Nwheat > MONICA > COUP > EPIC >
311 MCWLA > DailyDayCent. For silage maize aboveground biomass the order is: HERMES >
312 LandscapeDNDC > AquaCrop4.0 > DailyDayCent > SIMPLACE<LINTUL5> > STICS > APSIM(modified) >
313 MONICA > EPIC > APSIM.

314

315 **Aggregation effect - crop model interaction with space.** Differences in the interaction between
316 models and the choice of the sub-region did not show a clear trend (data not shown). However, the
317 proportion of crop models where the aggregation effects followed the order of the resolution was
318 lower in the sub-regions (*P*: 18.3 %, 21.8 % and 26.6 % for C0:R4, C1:R3 and z50, respectively).

319

320 **Aggregation effect - crop model interaction with production situation.** Crop models differed in their
321 sensitivity to climate input data aggregation across production situations (Table 3 and 4). While most
322 models showed no clear trend, aggregation effects followed a specific order in the case of few
323 models: increasing limitations led to more positive aggregation effects in HERMES and
324 LandscapeDNDC for both winter wheat and silage maize and for MONICA in the case of silage maize,
325 whereas APSIM and APSIM(modified) were not altered for both winter wheat and silage maize and
326 MCWLA in the case of winter wheat. For the crops simulated, aggregation effects of
327 SIMPLACE<LINTUL5>, DailyDayCent, COUP and Apsim-NWheat decreased with increasing limitation
328 in the production situation whereas STICS, EPIC and AquaCrop did not alter or showed an increasing
329 range.

330

331 **3.5) Systematic effects in crop model output due to climate input data aggregation and variable** 332 **importance**

333 Using differences in climate variables and their spatial variances as independent variables for PLS-
334 regression led to model-specific sets of variables which are most determinant for single year
335 aggregation effects when wheat or silage maize yield are simulated (Tables 3 and 4). The explained
336 variance by PLS varied between crops, models and production situations. For instance, the explained
337 variance was 60, 91 and 82 % of the single year aggregation effects in the wheat yields simulated by
338 LandscapeDNDC for potential, water-limited and nitrogen-water-limited production, respectively,
339 whereas SIMPLACE<LINTUL5> showed an opposite trend with 80, 61 and 54 %, respectively. Other
340 models showed constantly high (HERMES, 73 to 80 %) or mid (STICS, 59 to 61 %) ranges of explained
341 variance in aggregation effects of simulated wheat yields.

342 Key variables that statistically explained the variance for aggregation effects of single years were
343 identified by the variable importance for projection (VIP). Concerning winter wheat yield, most
344 models showed the highest VIP for variables related to radiation, followed by variables related to

345 temperature (e.g. HERMES) or again radiation (e.g. STICS, COUP, APSIM). Changes in the aggregation
346 effects of wheat yields of STICS for instance are apparently driven mainly by radiation in the period
347 before anthesis, followed by the temperature before anthesis. Few models indicated precipitation-
348 related terms as most important, mainly for water-limited and nitrogen-water-limited runs
349 (SIMPLACE<LINTUL5>, LandscapeDNDC, EPIC, MONICA). For silage maize, the climate variables with
350 the highest VIP to explain aggregation effects are precipitation- and temperature-related variables,
351 and less related to radiation. Furthermore, while changes in aggregation effects in winter wheat
352 were mainly related directly to changes in climate variables, changes in aggregation effects in silage
353 maize were related mainly to changes in the spatial variance of individual climate variables. No clear
354 trend was obtained for the importance of model outputs (Tables S1 and S2) to explain the effects of
355 climate input aggregation on either wheat or silage maize yields.

356

357 (Figure 3)

358 (Figure 4)

359 (Figure 5)

360 (Figure 6)

361 (Figure 7)

362 (Table 2)

363 (Table 3)

364 (Table 4)

365

366

367 **4) Discussion**

368 **4.1) Data aggregation effects on regional climate**

369 As expected for homogeneous data, changes in the climate variables due to spatial aggregation did
370 not alter the regional mean significantly, but decreased the spatial variance and the semivariance
371 while narrowing extremes. The range estimated from semivariograms was above or in the range of
372 the largest spatial resolution investigated. Thus, the requirement of aggregating data of spatial
373 coherence was met. However, aggregation effects at resolutions coarser than 100 km were not
374 investigated. Thus, without further analysis and depending on the research question, averaging
375 climate variables should probably be restricted to spatial resolutions up to the semivariogram range,
376 which was 94 to 162 km in this study depending on the climate variable. Climate input data
377 aggregation up to 100 km is supported by Van Bussel et al. (2011) and Angulo et al. (2013).

378 **4.2) General effects of climate input data aggregation on regional mean simulated yields and** 379 **biomass**

380 Simulated regional winter wheat and silage maize yields (mean of region and years) were biased
381 when using aggregated climate input data. However, aggregation effects were small compared to
382 the effect of production situations, year-to-year variability or variations across crop models.
383 Aggregation effects in mean yields up to 0.2 t ha⁻¹ as compared to 1 km grid cells are in line with
384 findings of Folberth et al. (2012) who found a decrease in mean yields of approximately 0.18 t ha⁻¹ of
385 maize after aggregating input data from approximately 7.5 to 45 km. Also Angulo et al. (2013) found
386 biases in the median yield of up to 0.26 t ha⁻¹ (LINTUL-SLIM) and 0.21 t ha⁻¹ (WOFOST) due to the use
387 of input data with resolutions ranging from 10 to 100 km, while biases from other models were
388 lower (<0.08 t ha⁻¹). Thus, aggregation effects on crop yields are on average low in all studies.

389 Our results show that aggregation hardly influenced the mean climate conditions, but decreased the
390 variance of the climate data. Consequently, an impact on crop model outputs was expected through
391 non-linear functions in the models. The low overall aggregation effect can however be explained as
392 follows. Firstly, the present study is situated in a region with a humid, temperate climate favourable
393 for crop growth and all simulation runs used a typical cropland soil with high water retention
394 capacity. Thus, changes in present climate extremes only slightly influenced the simulated mean
395 regional yield. Secondly, aggregation effects may partially cancel out (Rastetter et al. 1992) at the
396 grid cell level when several climate input variables are aggregated simultaneously and at the regional
397 level when effects of single grid cells cancel out over the region. However aggregation effects have
398 an impact at the grid cell level or on spatial patterns (Zhao et al. 2014a), which was also observed in
399 our study. In conclusion, the low biases in simulating mean crop yields improve the confidence in
400 applying crop models across scales for mean yield estimates of a given region in humid temperate
401 conditions. However, the remaining biases still add to the simulation error and they are likely to
402 increase with climate data variance and absolute level, increasing aridity of climate conditions,
403 model complexity and sensitivity, whenever non-linear effects do not cancel out. This mean
404 aggregation effect may therefore be best observed in stress situations as well as under near-
405 optimum conditions.

406 Unlike the mean, yield variance and distribution narrowed down in this study with aggregation. This
407 is partially in contrast to Angulo et al. (2013), who found the range of the yield distribution to be
408 only marginally influenced by spatial resolution of climate input variables. However, the Angulo et al.
409 study was based on climate data of a relatively topographically uniform region in south-western
410 Finland with humid climate conditions. Thus, the discrepancies between influences of aggregation

411 effects for the two regions (NRW and south-western Finland) on yield distributions are explained by
412 the spatial variance of the climate.

413 **4.3) Crop model-specific sensitivity to input climate data aggregation**

414 **Aggregation effect interaction of crop model and crop.** Despite an overall low bias in mean
415 simulated yield or biomass over the region due to climate input aggregation, the presented results
416 showed differences in the model response. For silage maize biomass, some models showed lower
417 sensitivity to the climate input aggregation (e.g. MONICA, effect in maize biomass: $<1 \text{ t ha}^{-1}$),
418 whereas other models showed stronger aggregation effects of up to 1.9 t ha^{-1} , (HERMES, APSIM).
419 Although most models showed nearly equally positive and negative aggregation effects, only in a
420 few models the aggregation effect had a dominant direction over all spatial resolutions (e.g.
421 dominant negative effect of input data aggregation in STICS, SIMPLACE<LINTUL5>). It is
422 questionable, whether these responses are the result of the model structure, or whether they result
423 from model parameterizations. Finally, major differences were found between crops regarding the
424 climate variables, which explain most of the variance of the single year aggregation effects (radiation
425 for winter wheat, temperature for silage maize). The variance in the aggregation effects were
426 explained in most models to approx. 60 % and in few occasions up to $>80 \%$ by PLS. While the crop
427 model structure does not change largely between simulating winter wheat and silage maize, these
428 changes in the model sensitivity again emphasize the role of model settings for the aggregation
429 effects.

430
431 **Aggregation effect interaction of crop model and time.** Analysis of the aggregation effects at single-
432 model- and single-year level (figures S2 and S4a – S4f) did not reveal general trends, but underlined
433 the high variability in model responses to climate input data aggregation. It can thus be concluded
434 that the year-to-year variability of yields masks the aggregation effects on long-term simulated
435 yields.

436
437 **Aggregation effect interaction of crop model and production situation.** Models reacted differently,
438 depending on the production situation. While the minimum and maximum aggregation effects of
439 AquaCrop4.0 showed a threefold increase from potential to water-limited production, no trend was
440 found across production situations with DailyDayCent, APSIM_modified and SIMPLACE<LINTUL5>.
441 However, some models (HERMES, LandscapeDNDC, Monica, EPIC) showed a tendency towards
442 larger negative aggregation effects on silage maize biomass when comparing potential and limited
443 production. Interestingly, the variance in aggregation effects explained by PLS decreased with
444 increasing limitations in the production situation, being on average 70.3, 62.8 and 60.9 % for winter
445 wheat and 57.9, 52.1 and 50.3 % for silage maize under potential, water-limited and nitrogen-water-
446 limited conditions. This indicates that increasing model complexity by adding sub-routines to
447 account for additional processes potentially increases the fraction of aggregation effects, which can
448 be regarded as not systematic, i.e. residual variability or noise. Angulo et al. (2013) proposed model-
449 specific fingerprints in the form of yield probability density functions (PDFs) after finding larger
450 discrepancies between models than between aggregation levels.

451 While no characteristic fingerprints were found for soil input data aggregation (Angulo et al. 2014),
452 the model-specific fingerprints remain to be validated for climate input data aggregation. Since the
453 model fingerprint certainly is modulated by the model structure, it may be co-determined by further
454 factors like model parametrization. Considering the different aggregation effects from similar
455 models (Supplementary 2: Apsim, Apsim_modified and Apsim-NWheat), aggregation effects seem to
456 be partly the result of model parametrization. This does not support the hypothesis of model-
457 specific fingerprints (Angulo et al. 2013). This is similar to the findings by Gardner et al. (1982), who

458 assumed – after testing hypothetical models of varying structure - that the level of complexity does
459 not alter the aggregation effect noticeably. Consequently, climate data aggregation effects cannot
460 directly be attributed to a given process when using regional, ensemble or other pooled outputs (e.g.
461 mean of years). The processes causing the aggregation effects must thus be assessed at the process
462 level, before generalizing the findings at coarser scales.

463

464 **Model-specific drivers for aggregation effects.** PLS-regression was used to identify possible drivers
465 of the aggregation effects on mean simulated yields, which were largely masked by the spatial and
466 temporal variance. However, possible model candidates for further analysis could be identified
467 since: 1) The explained variance by PLS shows which models exhibit systematic aggregation effects
468 explainable by a low number of factors, 2) the selected predictors identified climate variables and
469 model outputs as relevant key drivers. While the variance in aggregation effects for HERMES for
470 instance were explained by >70 % by PLS, this was only approx. 50 % for DailyDayCent. Similar
471 results were obtained with generalized linear models (GLM, data not shown). Thus, models differ not
472 only in their sensitivity, but also in their systematic component of aggregation effects. However, no
473 clear general trend distinguishing crop models in their drivers for aggregation effects was found.
474 While few models were identified as being influenced more by e.g. temperature or radiation, the
475 attribution of these variables to processes in the model remain to be interpreted. For instance,
476 HERMES showed aggregation effects well approximated by the duration of the growing period,
477 which itself largely depends on crop specific parameters (temperature sum, base temperature).
478 Although the structure of the models is known, a direct attribution of aggregation effects to the
479 model structure (supplement 2) fails due to the high variability of the effects. For instance,
480 aggregation effects on average were larger for i) simple light interception approaches than for
481 detailed approaches, ii) models accounting for vernalization than models not considering
482 vernalization, iii) yield formation based on harvest index than for yield formation based on other
483 approaches (e.g. partitioning during reproductive stages). Hence, for a deeper understanding of
484 aggregation effects and causal processes the analysis needs to be combined with other multivariate
485 methods (e.g. pattern recognition).

486

487 **4.6) Generalization of findings towards the assessment of aggregation effects**

488

489 Following Pierce et al. (1995) and Rastetter et al. (1992), the aggregation effect should increase with
490 increasing variance of the input data. Larger climate variability as well as different average climate
491 conditions could lead to different aggregation effect distributions especially under growth limiting
492 conditions. While this depends on the data (type, spatial heterogeneity) it is unknown how the
493 aggregation effects from climate data compare to those from other data types. Most of the spatial
494 yield variability in Germany is caused by soil properties and its interactions with climate. In order to
495 focus solely on climate data aggregation effects, soil was not considered as a factor in this study.
496 Aggregation effects from soil properties may therefore differ (Angulo et al. 2014) from the present
497 findings. Pierce et al. (1995) compared the contributions of aggregated input data to the resulting
498 bias in simulated net primary production, which was by 32 % due to spatially averaging climate data
499 (topography 32 %, vegetation and soils 34 %). This remains to be verified for crop models.

500

501 **5) Conclusions**

502 Spatial aggregation of climate input data caused considerable aggregation effects for single models
503 and in single years. Simulated regional yield estimates (average of region and years) were less
504 affected. Differences in simulated mean regional yields across models and/or production situations

505 or in single year yields were larger than the aggregation error. The mean aggregation effects across
506 models and years of up to 0.2 t ha⁻¹ (<3 %) contribute to the uncertainty of the estimate of regional
507 yield and biomass. Nevertheless, it has been shown that the effects are systematic. Crop models
508 differ in their sensitivity to aggregated data, showing different means and distributions of
509 aggregation effects, which also depend on the production situation and the crop. Crop models differ
510 in their systematic component of aggregation effects, regardless of the extent of the aggregation
511 effect. Aggregation effects can be attributed to different sources, including climate, climate
512 variability and model structure. Having studied a region in which precipitation rarely limits crop
513 growth, global radiation and temperature were identified as the relevant climate variables, which
514 strongly influence the aggregation effects on winter wheat and silage maize yields, respectively.

515 **6) Acknowledgment**

516 This study was supported by the BMBF/BMELV project on "Modeling European Agriculture with
517 Climate Change for Food Security (MACSUR)" (grant no. 2812ERA115). The work was partly
518 supported by the Swedish Research Council for Environment, Agricultural Sciences and Spatial
519 Planning and by strategic funding ("Soil-Water-Landscape") from the faculty of Natural Resources
520 and Agricultural Sciences (Swedish University of Agricultural Sciences). We thank ACCAF for financial
521 support and Record team (Eric Casellas) for technical support. We thank the Landesbetrieb
522 Information und Technik Nordrhein-Westfalen for providing regional yield data, and the German
523 Meteorological Service for providing weather data. We thank Professor Per-Erik Jansson (Royal
524 Institute of Technology in Stockholm) for valuable advice linked to the application of the Coup-
525 model. E. Teixeira thanks the Royal Society of New Zealand and the Climate Change Impacts and
526 Implications project for New Zealand (CCII) for financial support to collaborate with the INRES group
527 at the University of Bonn. S. Asseng and D. Cammarano acknowledge support from NOAA-RISA and
528 IFPRI.

529 **7) References**

- 530
- 531 Angulo C, Rötter R, Trnka M, Pirttioja N, Gaiser T, Hlavinka P, Ewert F (2013) Characteristic
532 'fingerprints' of crop model responses data at different spatial resolutions to weather input. *Eur J*
533 *Agron* 49: 104-114
- 534
- 535 Angulo C, Gaiser T, Rötter RP, Børgesen CD, Hlavinka P, Trnka M, Ewert F (2014) 'Fingerprints' of four
536 crop models as affected by soil input data aggregation. *Eur J Agron* 61: 35 – 48
- 537
- 538 Artan GA, Neale CMU, Tarboton DG (2000) Characteristic length scale of input data in distributed
539 models: implications for modeling grid size. *J Hydrol* 227: 128-139
- 540
- 541 Asseng S, Jamieson PD, Kimball B, Pinter P, Sayre K, Bowden JW, Howden SM (2004) Simulated
542 wheat growth affected by rising temperature, increased water deficit and elevated atmospheric
543 CO₂. *Field Crop Res* 85: 85-102
- 544
- 545 Asseng S, Keating BA, Fillery IRP, Gregory PJ, Bowden JW, Turner NC, Palta JA, Abrecht DG (1998)
546 Performance of the APSIM-wheat model in Western Australia. *Field Crop Res* 57: 163-179
- 547
- 548 Bahrenberg G, Giese E, Mevenkamp N, Nipper J (2010) *Statistische Methoden in der Geographie.*
549 *Band 1. Univariate und bivariate Statistik.* Borntraeger Science Publishers. Stuttgart. p. 86.
- 550

551 Bergez JE, Chabrier P, Gary C, Jeuffroy MH, Makowski D, Quesnel G, Ramat E, Raynal H, Rousse N,
552 Wallach D, Debaeke P, Durand P, Duru M, Dury J, Faverdin P, Gascuel-Odoux C, Garcia F (2013) An
553 open platform to build, evaluate and simulate integrated models of farming and agro-ecosystems.
554 *Environ Modell Softw* 39: 39–49
555

556 Bormann H, Breuer L, Graeff T, Huisman JA, Croke B (2009) Assessing the impact of land use change
557 on hydrology by ensemble modelling (LUCHEM) IV: Model sensitivity to data aggregation and spatial
558 (re-)distribution. *Advances in Water Resources* 32: 171-192
559

560 Brisson N, Mary B, Ripoche D, Jeuffroy MH, Ruget F, Nicoullaud B, Gate P, Devienne-barret F, Recous
561 S, Tayot X, Plenet D, Cellier P, Mached J, Marc J, Delécolle R (1998) STICS : a generic model for the
562 simulation of crops and their water and nitrogen balances . 1. Theory and parameterization applied
563 to wheat and corn. *Agronomie* 18: 311–346
564

565 Brisson N, Launay M, Mary B, Beaudoin N (2008) Conceptual basis, formalisations and
566 parameterization of the STICS crop model, Quae. ed.
567

568 Brown DG, Bian L, Walsh SJ (1993) Response of a distributed watershed erosion model to variations
569 in input data aggregation levels. *Computers & Geosciences* 19: 499-509
570

571 Cale WG, Oneill RV (1988) Aggregation and consistency problems in theoretical-models of
572 exploitative resource competition. *Ecol Model* 40: 97-109
573

574 Cale WG, Oneill RV, Gardner RH (1983) Aggregation error in non-linear ecological models. *Journal of*
575 *Theoretical Biology*, 100(3), 539-550
576

577 Chen C, Wang E, Yu Q (2010) Modeling wheat and maize productivity as affected by climate variation
578 and irrigation supply in North China Plain. *Agron J* 102: 1037-1049
579

580 Chipanshi AC, Ripley EA, Lawford RG (1998) Large-scale simulation of wheat yields in a semi-arid
581 environment using a crop-growth model. *Agr Syst* 59: 57-66
582

583 Cologne district council (2013) Nordrhein-Westfalen in Zahlen und Geodaten. URL: [www.bezreg-
584 koeln.nrw.de/brk_internet/publikationen/abteilung07/pub_geobasis_nrw.pdf](http://www.bezreg-koeln.nrw.de/brk_internet/publikationen/abteilung07/pub_geobasis_nrw.pdf) (last fetch:
585 15.12.2014).
586

587 Conrad Y, Fohrer N (2009) Modelling of nitrogen leaching under complex winter wheat and red
588 clover crop rotation on a drained agricultural field. *Physics and Chemistry of the Earth* 34: 530-540
589

590 Del Grosso SJ, Parton WJ, Mosier AR, Hartman MD, Brenner J, Ojima DS, Schimel DS (2001)
591 Simulated interaction of carbon dynamics and nitrogen trace gas fluxes using the DAYCENT model.
592 In: Schaffer M (Ed.), *Modeling Carbon and Nitrogen Dynamics for Soil Management*. CRC Press, Boca
593 Raton, Florida, USA, pp. 303–332.
594

595 Del Grosso SJ, Parton W, Mosier AR, Walsh MK, Ojima D, Thornton PE (2006) DAYCENT national scale
596 simulations of N₂O emissions from cropped soils in the USA. *J. Environ. Qual.* 35: 1451–1460
597

598 De Wit AJW, Boogaard HL, Van Diepen CA (2005) Spatial resolution of precipitation and radiation:
599 The effect on regional crop yield forecasts. *Agr Forest Meteorol* 135: 156-168
600

601 Evans LT, Fisher RA (1999) Yield potential: Its definition, measurement, and significance. *Crop*
602 *Science* 39: 1544-1551
603

604 Ewert F, Van Ittersum MK, Heckelei T, Therond O, Bezlepikina I, Andersen E (2011) Scale changes and
605 model linking methods for integrated assessment of agri-environmental systems
606

607 Folberth C, Yang H, Wang X, Abbaspour KC (2012) Impact of input data resolution and extent of
608 harvested areas on crop yield estimates in large-scale agricultural modeling for maize in the USA.
609 *Ecol Model* 235: 8-18
610

611 Gardner RH, Cale WG, Oneill RV (1982) Robust analysis of aggregation error. *Ecology* 63: 1771-1779
612

613 Gong X, Barnston AG, Ward MN (2003) The Effect of Spatial Aggregation on the Skill of Seasonal
614 Precipitation Forecasts. *J Climate* 16, 3059-3071
615

616 Guo L, Dai J, Ranjitkar S, Xu J, Luedeling E (2013) Response of chestnut phenology in China to climate
617 variation and change. *Agr Forest Meteorol* 180: 164-172
618

619 Haas E, Klatt S, Fröhlich A, Werner C, Kiese R, Grote R, Butterbach-Bahl K (2012) LandscapeDNDC: A
620 process model for simulation of biosphere-atmosphere-hydrosphere exchange processes at site and
621 regional scale. *Landscape Ecology*; DOI: 10.1007/s10980-012-9772-x
622

623 Hansen JW, Challinor A, Ines A, Wheeler T, Moron V (2006) Translating climate forecasts into
624 agricultural terms: advances and challenges. *Clim Res* 33: 27-41
625

626 Hansen JW, Jones JW (2000) Scaling-up crop models for climate variability applications. *Agr Syst* 65:
627 43-72
628

629 Heuvelink GBM, Pebesma EJ (1999) Spatial aggregation and soil process modelling. *Geoderma* 89:
630 47-65
631

632 Hoffmann H, Rath T (2012) Meteorologically consistent bias correction of climate time series for
633 agricultural models. *Theoretical and Applied Climatology* 110: 129-141
634

635 Hoffmann H, Rath T (2013) Future Bloom and Blossom Frost Risk for *Malus domestica* Considering
636 Climate Model and Impact Model Uncertainties. *Plos One* 8 (10). doi: 10.1371/journal.pone.0075033
637

638 Holzworth DP, Huth NI, De Voil PG, Zurcher EJ, Herrmann NI, McLean G, Chenu K, Van Oosterom EJ,
639 Snow V, Murphy C, Moore AD, Borwn H, Whish JPM, Verrall S, Fainges J, Bell LW, Peake AS, Poulton
640 PL, Hochman Z, Thorburn PJ, Gaydon DS, Dalgliesh NP, Rodriguez D, Cox H, Chapman S, Doherty A,
641 Teixeira E, Sharp J, Cichota R, Vogeler I (2014) APSIM – Evolution towards a new generation of
642 agricultural systems simulation. *Environ Model Softw* 62: 327-350
643

644 Jansson PE, Karlberg L (2004) Coupled heat and mass transfer model for soil-plant-atmosphere
645 systems, Royal Institute of Technology, Department of Civil and Environmental Engineering,
646 Stockholm, Sweden, 435 pp. , URL:

647 <http://www2.lwr.kth.se/Vara%20Datorprogram/CoupModel/NetHelp/default.htm> (last fetch:
648 15.12.2014)
649

650 Jones CA, Kiniry JR (1986) CERES-Maize: A simulation model of maize growth and development.
651 Texas A&M University Press, College Station, Texas, 194
652

653 Keating BA, Carberry PS, Hammer GL, Probert ME, Robertson MJ, Holzworth DP, Huth NI, Hargreaves
654 G, Meinke H, Hochman Z, Maclean G, Verburg K, Snow V, Dimes JP, Silburn M, Wang E, Brown S,
655 Bristow KL, Asseng S, Chapman SC, McCown RL, Freebairn DM, Smith CJ (2003) An overview of
656 APSIM, a model designed for farming systems simulation. *Eur J Agron* 18: 267-288
657

658 Ershadi A, McCabe MF, Evans JP, Walker JP (2013) Effects of spatial aggregation on the multi-scale
659 estimation of evapotranspiration. *Remote Sens Environ* 131, 51-62
660

661 Haverkamp S, Fohrer N, Frede HG (2005) Assessment of the effect of land use patterns on hydrologic
662 landscape functions: a comprehensive GIS-based tool to minimize model uncertainty resulting from
663 spatial aggregation. *Hydrol Process* 19, 715-727
664

665 Kersebaum KC (2007) Modelling nitrogen dynamics in soil-crop systems with HERMES. *Nutrient*
666 *cycling in agroecosystems* 77: 39-52
667

668 Kersebaum KC (2011) Special features of the HERMES model and additional procedures for
669 parameterization, calibration, validation, and applications In: L.R. Ahuja and L. Ma (ed.): *Advances in*
670 *Agr Syst Modeling Series 2*: 65-94
671

672 Kraus D, Weller S, Klatt S, Haas E, Wassmann R, Kiese R, Butterbach-Bahl K (2014) A new
673 LandscapeDNDC biogeochemical module to predict CH₄ and N₂O emissions from lowland rice and
674 upland cropping systems. *Plant Soil* 386: 125-149
675

676 Leopold U, Heuvelink GBM, Tiktak A, Finke PA, Schoumans O (2006) Accounting for change support
677 in spatial accuracy assessment of modelled soil mineral phosphorus concentration. *Geoderma* 130:
678 368-386
679

680 Littleboy M, Silburn D, Freebairn D, Woodruff D, Hammer G, Leslie J (1992) Impact of soil erosion on
681 production in cropping systems. I. Development and validation of a simulation model. *Soil Res* 30:
682 757-774
683

684 Lorite IJ, Mateos L, Fereres E (2005) Impact of spatial and temporal aggregation of input parameters
685 on the assessment of irrigation scheme performance. *J Hydrol* 300, 286-299
686

687 Luedeling E, Gassner A (2012) Partial Least Squares Regression for analyzing walnut phenology in
688 California. *Agr Forest Meteorol* 158: 43-52
689

690 Meentemeyer V (1989) Geographical perspectives of space, time, and scale. *Landscape Ecol* 3: 163-
691 173
692

693 Minsasny B, McBratney AB (2005) The Matérn function as general model for soil variograms.
694 *Geoderma* 128: 192-207

695
696 Nendel C, Berg M, Kersebaum KC, Mirschel W, Specka X, Wegehenkel M, Wenkel KO, Wieland R
697 (2011) The MONICA model: Testing predictability for crop growth, soil moisture and nitrogen
698 dynamics. *Ecol Model* 222: 1614-1625
699
700 Nendel C, Wieland R, Mirschel W, Specka X, Guddat C, Kersebaum KC (2013) Simulating regional
701 winter wheat yields using input data of different spatial resolution. *Field Crop Res* 145: 67-77
702
703 Nungesser MK, Joyce LA, McGuire AD (1999) Effects of spatial aggregation on predictions of forest
704 climate change response. *Climate Res* 11: 109-124
705
706 O'Neill RV (1977) Transmutations across hierarchical levels. Conference: Symposium on statistical
707 ecology, College Station, Texas, USA, 25 Jul 1977. OSTI ID: 7083394. Report Number(s): CONF-
708 770730-1, TRN: 77-018130
709
710 Parton WJ, Holland EA, Del Grosso SJ, Hartman MD, Martin RE, Mosier AR, Ojima DS, Schimel DS
711 (2001) Generalized model for NO_x and N₂O emissions from soils. *J. Geophys. Res.* 106: 17403-17420
712
713 Pierce LL, Running SW (1995) The effects of aggregating subgrid land-surface variation on large-scale
714 estimates of net primary production. *Landscape Ecology* 10: 239-253
715
716 Raes D, Steduto P, Hsiao TC, Fereres E (2009) AquaCrop-the FAO crop model to simulate yield
717 response to water: ii. Main algorithms and software description. *Agron J* 101: 438-447
718
719 Rastetter EB, King AW, Cosby BJ, Hornberger GM, Oneill RV, Hobbie JE (1992) Aggregating fine-scale
720 ecological knowledge to model coarser-scale attributes of ecosystems. *Ecol Appl* 2: 55-70
721
722 Shibu ME, Leffelaar PA, van Keulen H, Aggarwal PK (2010) LINTUL3, a simulation model for nitrogen-
723 limited situations: Application to rice. *Eur J Agron* 32: 255-271
724
725 Statistische Ämter des Bundes und der Länder (2013) Regionaldatenbank Deutschland.
726 <https://www.regionalstatistik.de/genesis/online/logon>, accessed 08/05/2014
727
728 Steduto P, Hsiao TC, Raes D, Fereres E (2009) AquaCrop-The FAO crop model to simulate yield
729 response to water: i. Concepts and underlying principles. *Agron J* 101: 426-437
730
731 Syphard AD, Franklin J (2004) Spatial aggregation effects on the simulation of landscape pattern
732 and ecological processes in southern California plant communities. *Ecol Model* 180, 21-40
733
734 Tao F, Yokozawa M, Zhang Z (2009) Modeling the Impacts of Weather and Climate Variability on
735 Crop Productivity over a Large Area: A New Process-based Model Development, Optimization, and
736 Uncertainties Analysis. *Agr Forest Meteorol* 149: 831-850
737
738 Tao F, Zhao Z (2013) Climate change, wheat productivity and water use in the North China Plain: A
739 new super-ensemble-based probabilistic projection. *Agr Forest Meteorol* 170: 146-166
740
741 Taylor KE (2001) Summarizing multiple aspects of model performance in a single diagram. *Journal of*
742 *Geophysical Research-Atmospheres* 106: 7183-7192

743

744 Van Bussel LGJ, Ewert F, Leffelaar PA (2011a) Effects of data aggregation on simulations of crop
745 phenology. *Agriculture Ecosystems & Environment* 142: 75-84

746

747 Van Bussel LGJ, Ewert F, Zhao G, Hoffmann H, Wallach D, Constantin J, Raynal H, Klein C, Biernath C,
748 Heinlein F, Tao F, Rötter R, Cammarano D, Asseng S, Elliott J, Glotter M, Nendel C, Kersebaum KC,
749 Specka X, Basso B, Baigorria GA, Romero C (2014) Spatial sampling of weather data for regional crop
750 yield simulations. *Agric For Met* (submitted)

751

752 Van Bussel LGJ, Muller C, van Keulen H, Ewert F, Leffelaar PA (2011b) The effect of temporal
753 aggregation of weather input data on crop growth models' results. *Agr Forest Meteorol* 151: 607-
754 619

755

756 Van Ittersum M, Leffelaar P, Van Keulen H, Kropff M, Bastiaans L, Goudriaan J (2003) On approaches
757 and applications of the Wageningen crop models. *Eur J Agron* 18: 201-234

758

759 Van Ittersum MK, Rabbinge R (1997) Concepts in production ecology for analysis and quantification
760 of agricultural input-output combinations. *Field Crop Res* 52: 197-208

761

762 Vanuytrecht E, Raes D, Steduto P, et al (2014) AquaCrop: FAO'S crop water productivity and yield
763 response model. *Environ Model Softw* 62:351–360. doi: 10.1016/j.envsoft.2014.08.005

764

765 Wackernagel H (1995) *Multivariate Geostatistics*, Springer.

766

767 Wang E, Robertson M, Hammer G, Carberry P, Holzworth D, Meinke H, Chapman S, Hargreaves J,
768 Huth N, McLean G (2002) Development of a generic crop model template in the cropping system
769 model APSIM. *Eur J Agron* 18: 121-140

770

771 Wang E, Zhao Z (2013) Improving APSIM for simulation of temperature response of wheat (APSIM-
772 -WheatE). In Alderman et al (ed). *Proceedings of the workshop Modeling Wheat Response to High*
773 *Temperature, CIMMYT, El Batan, Texcoco, Mexico, June 19-21, 2013.* p 29.

774

775 Webster R, Oliver M (2001) *Geostatistics for Environmental Scientists*. Wiley & Sons.

776

777 Weihermüller L, Huisman JA, Graf A, Herbst M, Vereecken H (2011) Errors in Modeling Carbon
778 Turnover Induced by Temporal Temperature Aggregation. *Vadose Zone Journal* 10: 195-205.

779

780 Williams JR (1995) The EPIC model. In: Singh V.P. (Ed.), *Computer models of watershed hydrology*.
781 *Water resources publications, Highland Ranch CO*, pp. 909-1000.

782

783 Wold S (1994) PLS for Multivariate Linear Modeling. In van de Waterbeemd H (Editor), *QSAR:*
784 *Chemometric Methods in Molecular Design. Methods and Principles in Medicinal Chemistry*.
785 *Weinheim, Verlag-Chemie*.

786

787 Wold S, Sjöström M, Eriksson L (2001) PLS-regression: a basic tool of chemometrics. *Chemometr*
788 *Intell Lab* 58: 109-130

789

790 Yeluripati JB, Van Oijen M, Wattenbach M, Neftel A, Ammann A, Parton WJ, Smith P (2009) Bayesian
791 calibration as a tool for initialising the carbon pools of dynamic soil models. *Soil Biology &*
792 *Biochemistry* 41: 2579–2583
793
794 Zhao G, Hoffmann H, Van Bussel LGJ, Enders A, Specka X, Sosa C, Yeluripati J, Tao FL, Constantin J,
795 Teixeira E, Grosz B, Doro L, Zhao Z, Nendel C, Kiese R, Raynal H, Eckersten H, Haas E, Wang E, Kuhnert
796 M, Trombi G, Bindi M, Lewan E, Bach M, Kersebaum KC, Rötter R, Roggero PP, Wallach D, Krauss G,
797 Siebert S, Gaiser T, Ewert F (2014a) Effect of weather data aggregation on regional crop simulation
798 for different crops, production conditions, and response variables. *Clim Res* (submitted)
799
800 Zhao G, Siebert S, Rezaei EE, Yan C, Ewert F (2014b) Demand for multi-scale weather data for
801 regional crop modelling. *Agr For Meteorol* (submitted)

802 **8) Appendix**

803 8.1) Tables

804 (Table 5)

805 (Table 6)

806 (Table 7)

807 8.2) Equations

808 **Grids.** We define a regular grid R (<http://spatialreference.org/ref/epsg/31467/>) with grid points

$$r = \{(\lambda_i; \phi_j) | \lambda_{i,j} - \lambda_{i-1,j} = \phi_{i,j} - \phi_{i,j-1} = \alpha\} \quad (1)$$

λ : gauss-krüger northing value [km]

ϕ : gauss-krüger easting value [km]

i, j : grid index [–]

α : resolution [km]

809

810 Grids of aggregated data were obtained by taking the spatial mean of data at $\alpha = 1$ km resolution:

$$\left. \begin{aligned} f_{\theta}^{\beta}(\mathbf{X}) &= \mathbf{X}' \text{ with} \\ \mathbf{X}' | x'_{s,z} &= \frac{\sum_{i=\beta(s-1)+1}^{i=\beta s} \sum_{j=\beta(z-1)+1}^{j=\beta z} x_{i,j}}{\beta^2} \end{aligned} \right\} \text{with} \quad (2)$$

X : grid to be aggregated ($\alpha=1$)

X' : aggregated grid

β : resolution after aggregation [km]

i, j : grid indices at $\alpha = 1$ km

s, z : grid indices at β

811

812 Five grids of resolutions of 1, 10, 25, 50 and 100 km with the corresponding number of grid cells
 813 34168, 20, 80, 24 and 9 were constructed. Empty grid cells (data unavailable) were ignored in the
 814 calculations. Having time series of daily time steps, f_{θ} was applied on each time step. The standard
 815 distance of the resulting grids, being a measure for the grid point dispersion (Bahrenberg et al.
 816 2010), is given by Fig. S1. Maps displaying main regional climate variables are given by Zhao et al.
 817 (2014a).

818 **Variable notation.** A simplified notation will be used in the following, indexing variables in their
 819 dimensions $\Omega = \{A_1, A_2 \dots A_k\}$. In the following, equations are conducted over all elements of a
 820 given dimension and are applied to all dimensions indicated. For instance, averages are given by

$$\mu_{A_1, A_2 \dots A_k}(x) =: \frac{1}{\prod_{k=1}^k A_k} \sum_{a_1=1}^{A_1} \sum_{a_2=1}^{A_2} \dots \sum_{a_k=1}^{A_k} x_{a_1, a_2 \dots a_k} \quad (3)$$

821

822 where the variable x is averaged over dimensions A . In the following, these dimensions were
 823 considered

$$\Omega' = \{\alpha, c, t, m\} \text{ where} \quad (4)$$

Ω' : dimension, array of dimensions

α : resolution [km]

c : grid cell [-]

t : time step [d],[yr]

824 m : crop model [-]

825 e.g. $Yield_{\alpha,c,t,m}$ refers to a yield of a given resolution, grid cell, year and crop model.

826 **Analysis of aggregation effects.** Mean aggregation effects were calculated as:

827

$$\Delta_{c,t}(x_\alpha) = \mu_{c,t}(x_{\alpha,c,t}) - \mu_{c,t}(x_{\alpha=1,c,t}) \text{ with} \quad (4)$$

$\Delta_{c,t}(x_\alpha)$: Aggregation effect for resolution α and variable x

c : grid cell [-]

t : time step [d], [yr]

828 α : resolution

829 Eq. 4 was applied on climate data with daily time steps (t , [d]) as well as on yearly yields (t , [yr]) of
830 each model. Consistently, having the spatial variance

$$\sigma^2(x_\alpha) = \mu_{c,t} \left(\left\{ x_{c,t,\alpha} - \mu_c(x_{c,t,\alpha}) \right\}^2 \right) \quad (5)$$

831

832 aggregation effects in the spatial variance were quantified as

$$\Delta(\sigma^2(x_\alpha)) = \sigma^2(x_\alpha) - \sigma^2(x_{\alpha=1}) \text{ with} \quad (6)$$

833

834 **Analysis of systematic effects in simulated yields.** The order of mean changes in a given model
835 output due to input data aggregation was analyzed by calculating the fraction of simulated yields
836 following monotonously the order of the resolutions for each model:

$$P = \mu(\gamma_t) \cdot 100, \text{ with}$$

$$\gamma_t = \begin{cases} 1 & \text{if } Y_{t,\alpha=100} > Y_{t,\alpha=50} > Y_{t,\alpha=25} > Y_{t,\alpha=10} > Y_{t,\alpha=1} \\ 1 & \text{if } Y_{t,\alpha=100} < Y_{t,\alpha=50} < Y_{t,\alpha=25} < Y_{t,\alpha=10} < Y_{t,\alpha=1} \\ 0 & \text{else} \end{cases}$$

$$Y_{\alpha,t} = \mu_c(x_{\alpha,c,t})$$

P : Percentage of yields following monotonously the order of resolutions α [%]

Y : Winter wheat grain yield of silage maize aboveground biomass [t ha⁻¹]

837 γ : counting variable

838 **Equations for Taylor diagrams.**

839 The centered root-mean-square difference (RMSD) was calculated as follows:

$$RMSD_m = \left[\frac{1}{N} \sum_{c,t,m} \left((x_{c,t,m} - \mu_{c,t}(x_{c,t,m})) - (\mu_m(x_{c,t,m}) - \mu_{m,c,t}(x_{c,t,m})) \right)^2 \right]^{1/2} \quad (8)$$

c : grid cell [-]

t : time step [yr]

m : model

840 N : 990872 (winter wheat), 1025040 (silage maize)

841 The standard deviation $\%$ for single models and for the model ensemble mean were calculated as
 842 described in eq. 5. The correlation coefficient R was calculated as follows:

$$R_m = \frac{\frac{1}{N} \sum_{c,t,m} (x_{c,t,m} - \mu_{c,t}(x_{c,t,m})) \cdot (\mu_m(x_{c,t,m}) - \mu_{m,c,t}(x_{c,t,m}))}{\mu_{c,t} \left(\left\{ x_{c,t,m} - \mu_c(x_{c,t,m}) \right\}^2 \right) \cdot \mu_{c,t} \left(\left\{ \mu_m(x_{c,t,m}) - \mu_{c,m}(x_{c,t,m}) \right\}^2 \right)} \quad (9)$$

843

844

845 **Tables**

846 Table 1. Climate of North-Rhine Westphalia (1982-2011, not area weighted). Standard deviations are
 847 calculated from all grid cells and years of a corresponding resolution.

Scale [km]	Annual precipitation sum		Mean daily temperature		Mean annual global radiation sum	
	Mean [mm yr ⁻¹]	σ [mm yr ⁻¹]	Mean [°C]	σ [°C]	Mean [MJ m ⁻² yr ⁻¹]	σ [MJ m ⁻² yr ⁻¹]
1	898.9	214.0	9.7	1.2	3758.0	169.4
10	881.7	204.0	9.6	1.2	3757.1	166.8
25	873.1	191.9	9.5	1.2	3756.6	163.8
50	853.8	170.8	9.4	1.1	3754.0	162.0
100	824.4	149.8	9.4	1.0	3765.5	160.6

848

849

850

851

852 Table 2. Impact of climate input data aggregation on model ensemble mean and spatial variance of
 853 simulated yields.

Production situation*	Scale [km]	Winter wheat grain yield		Silage maize aboveground biomass	
		mean [t ha ⁻¹]	σ^2 [t ha ⁻¹] ²	mean [t ha ⁻¹]	σ^2 [t ha ⁻¹] ²
P	1	8.6	0.3	17.4	4.2
P	10	8.6	0.3	17.4	3.8
P	25	8.6	0.2	17.4	3.3
P	50	8.6	0.2	17.5	2.5
P	100	8.7	0.1	17.6	1.5
W	1	8.2	0.5	16.2	4.1
W	10	8.2	0.5	16.1	3.7
W	25	8.3	0.4	16.2	3.2
W	50	8.3	0.3	16.3	2.4
W	100	8.4	0.2	16.4	1.6
N	1	7.6	0.4	15.5	4.0
N	10	7.6	0.4	15.4	3.6
N	25	7.6	0.3	15.5	3.1
N	50	7.6	0.2	15.6	2.3
N	100	7.7	0.2	15.7	1.6

855 * P: Potential; W: Water-limited; N: Nitrogen-water-limited

856

857 Table 3. Climate variables related to aggregation effects with winter wheat grain yield. Nomenclature: **d**: difference; **v**: spatial variance; **P**: precipitation
858 sum, **Tmin/Tmean/Tmax**: minimum, mean, maximum air temperature; **R**: global radiation sum; **GP**: growing period (=sowing to maturity); **SA**: sowing-to-
859 Anthesis; **AM**: anthesis-to-maturity; **L30A/L30M**: period of 30 days before anthesis, maturity. Examples: dRSA, difference in the global radiation sum from
860 sowing to anthesis; dvTminGP, difference in the spatial variance of the daily minimum temperature during the growing period. Variables are sorted from
861 one to five in the order of their variable importance.

Model	Production* Situation	Single year aggregation effect (difference in grain yield, [t ha ⁻¹])		Explained Variance	Variable 1	Variable 2	Variable 3	Variable 4	Variable 5
		minimum	maximum						
HERMES	P	-0.04	0.37	0.80	dRGP	dTminAM	dRL30A	dTmeanAM	dTmeanGP
HERMES	W	-0.14	0.57	0.73	dRGP	dvTmeanSA	dvTmeanGP	dTmeanGP	dvTmaxGP
HERMES	N	-0.13	0.58	0.74	dRGP	dvTmeanSA	dvTmeanGP	dTmeanGP	dvTmaxGP
MONICA	P	-0.33	0.47	0.75	dRGP	dvPSA	dvTmaxSA	dvTmeanSA	dvPGP
MONICA	W	-0.60	0.47	0.59	dvPSA	dvPGP	dTmaxSA	dvTmeanSA	dvTmaxSA
MONICA	N	-0.60	0.47	0.59	dvPSA	dvPGP	dTmaxSA	dvTmeanSA	dvTmaxSA
SIMPLACE<L5>	P	-0.06	0.37	0.80	dRSA	dRGP	dPL30A	dvTmeanSA	dvTminGP
SIMPLACE<L5>	W	-0.77	0.30	0.61	dvPGP	dvPSA	dTmeanSA	dvTmeanL30M	dvTminL30M
SIMPLACE<L5>	N	-0.73	0.37	0.54	dvPGP	dvPSA	dTmeanSA	dvTminL30M	dvTmeanL30M
STICS	P	-0.60	0.62	0.59	dRSA	dRL30A	dTmaxL30A	dRGP	dTmeanL30A
STICS	W	-0.58	0.58	0.61	dRSA	dRL30A	dTmaxL30A	dvTminGP	dvTmaxSA
STICS	N	-0.56	0.62	0.60	dRSA	dRL30A	dTmaxL30A	dTmeanL30A	dvTmaxSA
MCWLA	P	-0.72	0.73	0.64	dRSA	dRGP	dRL30A	dPGP	dvTmeanGP
MCWLA	W	-0.72	0.73	0.64	dRSA	dRGP	dRL30A	dPGP	dvTmeanGP
DayCent	P	-0.51	0.49	0.52	dRL30M	dvRL30M	dPL30M	dTminGP	dTmaxL30M
DayCent	W	-0.48	0.47	0.35	dPL30M	dvPGP	dTminL30M	dTmaxGP	dTmaxL30M
DayCent	N	-1.90	0.18	0.73	dRL30M	dRGP	dvTmaxGP	dvTmeanGP	dvRL30M
LandscapeDNDC	P	-2.36	0.17	0.60	dPL30M	dvPGP	dRL30M	dvPL30M	dvTmaxGP
LandscapeDNDC	W	-0.88	0.18	0.91	dPL30M	dvPGP	dRL30M	dvTmaxGP	dRGP
LandscapeDNDC	N	-0.70	0.49	0.82	dvPGP	dPL30M	dRL30M	dvPL30M	dvTmaxGP
COUP	P	-0.04	0.51	0.71	dRL30A	dRGP	dvTminGP	dRSA	dTmaxL30A
COUP	W	-0.48	0.30	0.45	dRSA	dRL30A	dRL30M	dvTminGP	dvPL30A
APSIM	P	-0.03	0.39	0.77	dRGP	dRSA	dvTmeanSA	dvTmaxSA	dTmeanSA

APSIM	W	-0.03	0.41	0.77	dRGP	dRSA	dvTmeanSA	dTmeanSA	dvTmaxSA
APSIM	N	-0.13	0.27	0.57	dRSA	dRGP	dRL30A	dvTmaxSA	dvTmeanSA
APSIM (modified)	P	-0.08	0.84	0.79	dRSA	dRGP	dTminAM	dvTmaxSA	dvTmeanGP
APSIM (modified)	W	-0.15	0.83	0.77	dRSA	dRGP	dTminAM	dvPSA	dvPGP
APSIM (modified)	N	-0.21	0.58	0.71	dRSA	dTminAM	dTmaxL30M	dvPGP	dRGP
EPIC	P	-0.02	0.24	0.73	dRGP	dvTminGP	dvRL30M	dTmeanGP	dRL30M
EPIC	W	-0.37	0.57	0.50	dRGP	dvTminGP	dvTmaxGP	dTmeanGP	dvTmeanGP
EPIC	N	-0.27	0.25	0.18	dvPGP	dvTminGP	dPGP	dvRL30M	dTmaxGP
APSIM-NWHEAT	P	-0.10	0.32	0.74	dTminAM	dPL30A	dRGP	dRSA	dRAM
APSIM-NWHEAT	W	-0.50	0.32	0.61	dvPSA	dvPGP	dTmaxL30M	dPL30M	dTmeanL30M

862 *P: Potential; W: Water-limited, N: Nitrogen-water-limited.

863

864

865 Table 4. Climate variables related to aggregation effects with silage maize. Nomenclature: **d**: difference; **v**: spatial variance; **P**: precipitation sum,
866 **Tmin/Tmean/Tmax**: minimum, mean, maximum air temperature; **R**: global radiation sum; **GP**: growing period (=sowing to maturity); **SA**: sowing-to-
867 Anthesis; **AM**: anthesis-to-maturity; **L30A/L30M**: period of 30 days before anthesis, maturity. Examples: dRSA, difference in the global radiation sum from
868 sowing to anthesis; dvTminGP, difference in the spatial variance of the daily minimum temperature during the growing period. Variables are sorted from
869 one to five in the order of their variable importance.

Model	Production* Situation	Single year aggregation effect (difference in grain yield, [t ha ⁻¹])		Explained Variance	Variable 1	Variable 2	Variable 3	Variable 4	Variable 5
		minimum	maximum						
HERMES	P	-0.15	1.42	0.85	dvPGP	dTminGP	dvTmaxGP	dPL30M	dTmaxGP
HERMES	W	-0.15	1.42	0.85	dvPGP	dTminGP	dvTmaxGP	dPL30M	dTmaxGP
HERMES	N	-0.06	1.97	0.83	dvTmaxGP	dvRL30M	dTminGP	dTminL30M	dvPGP
MONICA	P	-0.71	0.30	0.55	dvRL30M	dvTmeanL30M	dTmaxGP	dvTminL30M	dRGP
MONICA	W	-0.63	0.83	0.49	dTmaxGP	dvRL30M	dvPGP	dTmeanGP	dTminGP
MONICA	N	-0.63	0.83	0.49	dTmaxGP	dvRL30M	dvPGP	dTmeanGP	dTminGP
SIMPLACE<L5>	P	-1.24	0.68	0.49	dTmaxGP	dTminGP	dvTmaxGP	dvPGP	dPGP
SIMPLACE<L5>	W	-1.21	0.24	0.58	dTminGP	dvPGP	dvTmaxGP	dvRL30M	dTmaxGP
SIMPLACE<L5>	N	-1.20	0.42	0.46	dvPGP	dTmaxGP	dTminGP	dPL30M	dvRGP
STICS	P	-0.61	0.25	0.56	dvPGP	dTminL30M	dRL30M	dTminGP	dTmeanGP
STICS	W	-1.58	0.40	0.30	dvPGP	dRGP	dPL30M	dvRGP	dvRL30M
STICS	N	-1.58	0.42	0.29	dvPGP	dRGP	dvRGP	dPL30M	dvRL30M
DayCent	P	-0.71	1.07	0.52	dvPGP	dTmaxGP	dRL30M	dPGP	dTmeanGP
DayCent	W	-0.71	1.07	0.52	dvPGP	dTmaxGP	dRL30M	dPGP	dTmeanGP
DayCent	N	-0.71	1.07	0.52	dvPGP	dTmaxGP	dRL30M	dPGP	dTmeanGP
LandscapeDNDC	P	0.00	0.57	0.80	dvPGP	dvPL30M	dPL30M	dRGP	dvTmaxGP
LandscapeDNDC	W	0.00	0.60	0.79	dvPGP	dvPL30M	dPL30M	dvTmaxGP	dRGP
LandscapeDNDC	N	-0.11	0.90	0.71	dvPGP	dRGP	dPL30M	dvTmaxGP	dvPL30M
APSIM	P	-0.94	1.93	0.30	dPL30M	dTmaxGP	dTmeanL30M	dRGP	dTmaxL30M
APSIM	W	-0.81	1.93	0.29	dPL30M	dTmaxGP	dTmeanL30M	dRGP	dvPL30M
APSIM	N	-0.80	1.92	0.29	dPL30M	dTmaxGP	dTmeanL30M	dRGP	dvPL30M
APSIM (modified)	P	-1.00	1.48	0.41	dTmaxGP	dvPL30M	dTmeanL30M	dTmeanGP	dTminL30M
APSIM (modified)	W	-1.00	1.48	0.40	dTmaxGP	dvPL30M	dTmeanL30M	dTmeanGP	dvPGP

APSIM (modified)	N	-1.00	1.48	0.39	dTmaxGP	dvPL30M	dTmeanL30M	dTmeanGP	dTminL30M
EPIC	P	-0.30	0.80	0.57	dvRL30M	dvTminGP	dvTminL30M	dvTmeanGP	dRGP
EPIC	W	-1.04	0.98	0.55	dvRGP	dPGP	dPL30M	dvRL30M	dvTmaxGP
EPIC	N	-1.04	0.98	0.55	dvRGP	dPGP	dPL30M	dvRL30M	dvTmaxGP
AquaCrop4.0	P	-0.40	0.55	0.74	dPGP	dvRL30M	dvPL30M	dvRGP	dvTmaxGP
AquaCrop4.0	W	-1.26	1.99	0.44	dvTminGP	dvRL30M	dvPGP	dPGP	dRL30M

870 *P: Potential; W: Water-limited, N: Nitrogen-water-limited.

871 Table 5. Crop Models*.

No.	Model	References
1	APSIM-Nwheat	Asseng et al. 1998, 2004; Keating et al. 2003
2	APSIM	Keating et al. 2003, Holzworth et al. 2014
3	APSIM, modified	Chen et al. 2010; Keating et al. 2003; Wang et al. 2002
4	AquaCrop4.0	Raes et al. 2009; Steduto et al. 2009; Vanuytrecht et al. 2014
5	COUP	Conrad & Fohrer 2009; Jansson & Karlberg 2004
6	DailyDayCent	Del Grosso et al. 2001, 2006; Parton et al. 2001; Yeluripati et al. 2009
7	EPIC v. 0810	Williams 1995
8	HERMES	Kersebaum 2007, 2011
9	LandscapeDNDC	Haas et al. 2012, Kraus et al. 2014
10	LINTUL5	Van Ittersum et al. 2003; Shibu et al. 2010
11	MCWLA	Tao et al. 2009, 2013
12	MONICA	Nendel et al. 2011
13	STICS	Bergez et al. 2013; Brisson et al. 1998, 2008

872 * A more detailed description is given in the supplementary 2.

873

874

875 Table 6. Simulation runs conducted by models.

Factor	Level
Crop	Winter wheat, Silage Maize
Production situation	Potential ^a , Water-limited ^b , Nitrogen-water-limited ^c
Resolution [km]	1, 10, 25, 50, 100

876 ^a growth is limited by temperature and radiation.877 ^b growth is limited by precipitation, temperature and radiation878 ^c growth is limited by nitrogen, precipitation, temperature and radiation

879

880

881 Table 7. Crop model settings and assumptions.

Domain	Unit	Winter Wheat	Silage Maize
Sowing date	DOY ^a	274	110
Harvest date	DOY ^a	213	263
Average Yield ^b	t ha ⁻¹	7.2	14.3
Max. rooting depth	m	1.5	1.5
Time of ploughing	-	autumn	autumn
Planting density	m ⁻²	400	10
Sowing depth	m	0.04	0.06
Initial soil moisture relative to available field capacity ^c	%	50	80
Initial Nmin ^d	kg ha ⁻¹	56	56
Nitrogen fertilization	kg ha ⁻¹	130, 52, 26	30, 208
Date of fertilization	DOY ^a	60, 105, 152	91, 152

882 ^a Day of the year of a non-leap year. ^b Area weighted average yield derived from county statistics, moisture content: 0 %. ^c Set for each soil layer. ^d Total mineral Nitrogen of the soil profile. Values differ with soil layer.

885

886

887 **Figure Captions**

888 Fig. 1. Shape and elevation of the state of North-Rhine Westphalia, Germany. Squares display
889 selected areas used to validate results at state level.

890 Fig. 2. Illustration of climate data resolution $\alpha = 1::100$ [km] used as input for crop models.

891 Fig. 3. Area weighted mean and range of key climate variables as well as their spatial variance as
892 affected by data aggregation (Tmin, Tmean, Tmax: daily minimum, mean and maximum temperature
893 respectively). Values are average area means and extremes.

894 Fig. 4. Spatial dependency of selected climate variables in North-Rhine Westphalia. A) Empirical
895 semivariance (dots) and fitted variogram model (solid lines). A Gaussian model was fitted to daily
896 mean temperature (Tmean) and precipitation whereas an exponential model was used for global
897 radiation. B) Empirical semivariance (dots) and fitted Gaussian variogram model (solid lines) for
898 precipitation at varying resolutions α .

899 Fig. 5. Simulated winter wheat grain yield and silage maize aboveground biomass for three
900 production situations at 1 km resolution: Single model and observed 25 to 75 percentile range across
901 the region (shaded areas), model ensemble and observed area weighted mean from county-level
902 statistics (white lines). Areas are plotted with transparency, thus darker areas illustrate coinciding
903 simulation results of several models or coincidence of simulation results with observations.

904 Fig. 6. Probability density functions (pdf) of winter wheat grain yield and silage maize aboveground
905 biomass. Pdfs were estimated from mean grid cell yields and biomass (mean of years) using a
906 Gaussian kernel of bandwidth 0.1 and 0.3 t ha⁻¹ for winter wheat and silage maize, respectively.

907 Fig. 7. Taylor diagrams of simulated winter wheat and silage maize yields from respectively 29 and
908 30 years and from 34168 grid cells ($\alpha = 1$ km), showing: the standard deviation of each model (σ),
909 the correlation between the models (R) and the centered root mean square difference to the
910 ensemble mean (RMSD). Denser distributions show smaller diversity among models and vice versa.
911 RMSD and standard deviation are given in t ha⁻¹. For each model $n = 990,872$ and $n = 1,025,040$ for
912 winter wheat and silage maize, respectively.

913 Fig. 8. Differences of winter wheat grain yield and silage maize aboveground biomass simulated with
914 aggregated input climate data to yield and biomass simulated with climate time series at 1 km
915 resolution of North-Rhine Westphalia (NRW), two 100 km² subregions C0:R4 and C1:R3 and one
916 subregion, z50, consisting of five 50 km² grid cells (see Fig. 1 for regions). The figure displays the min-
917 to-max ranges over the models (shaded and hatched areas) and the ensemble median (thick lines).
918 Values are mean values of 1983 to 2011.

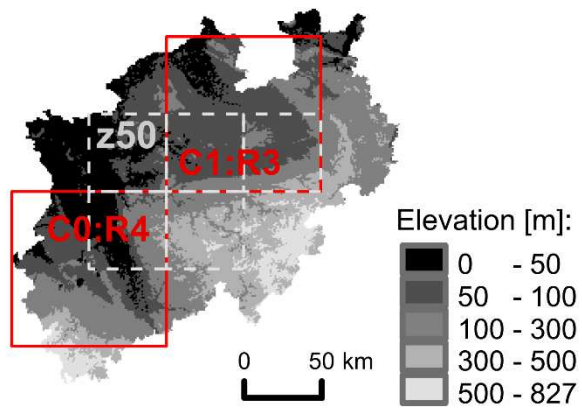
919

920

921

922 **Figures**

923



924

925 Fig.1

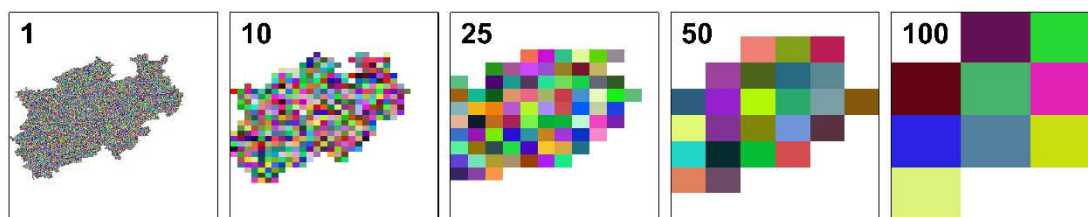
926

927

928

929

930

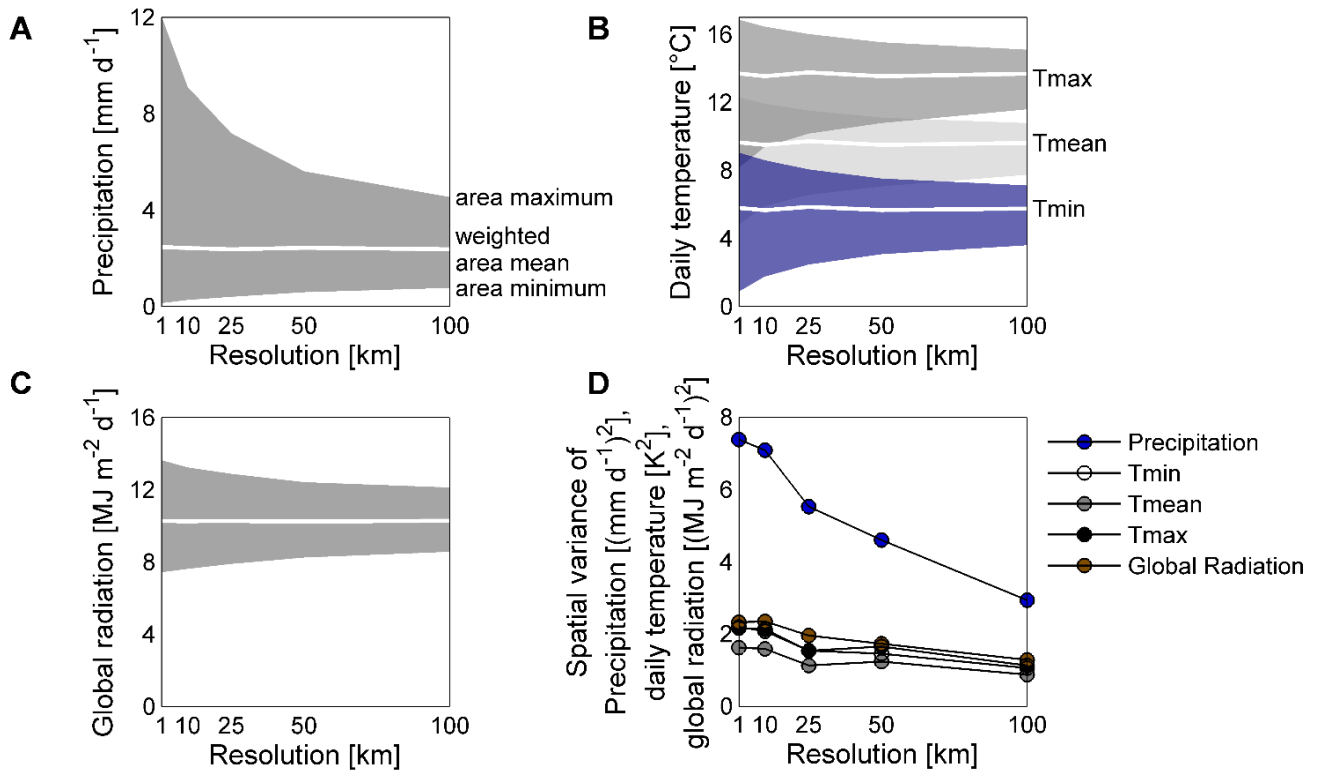


931

932 Fig.2

933

934



935

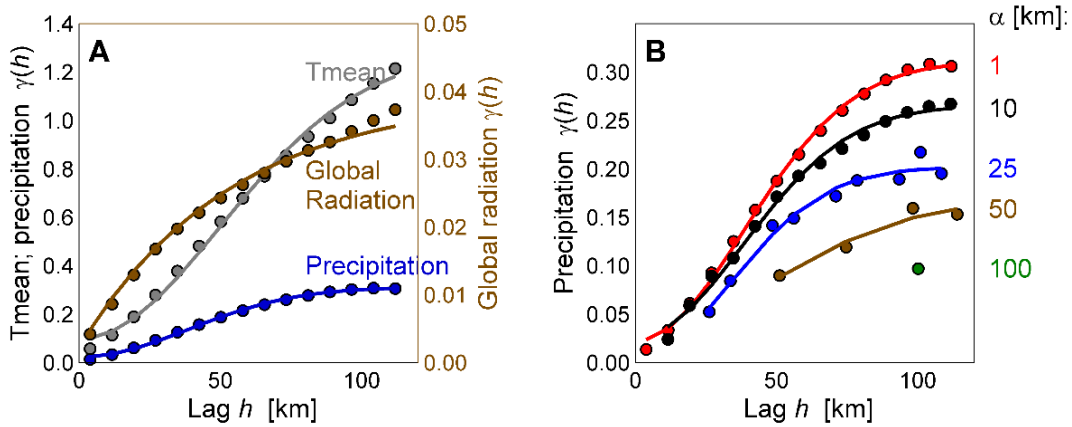
936 Fig. 3

937

938

939

940



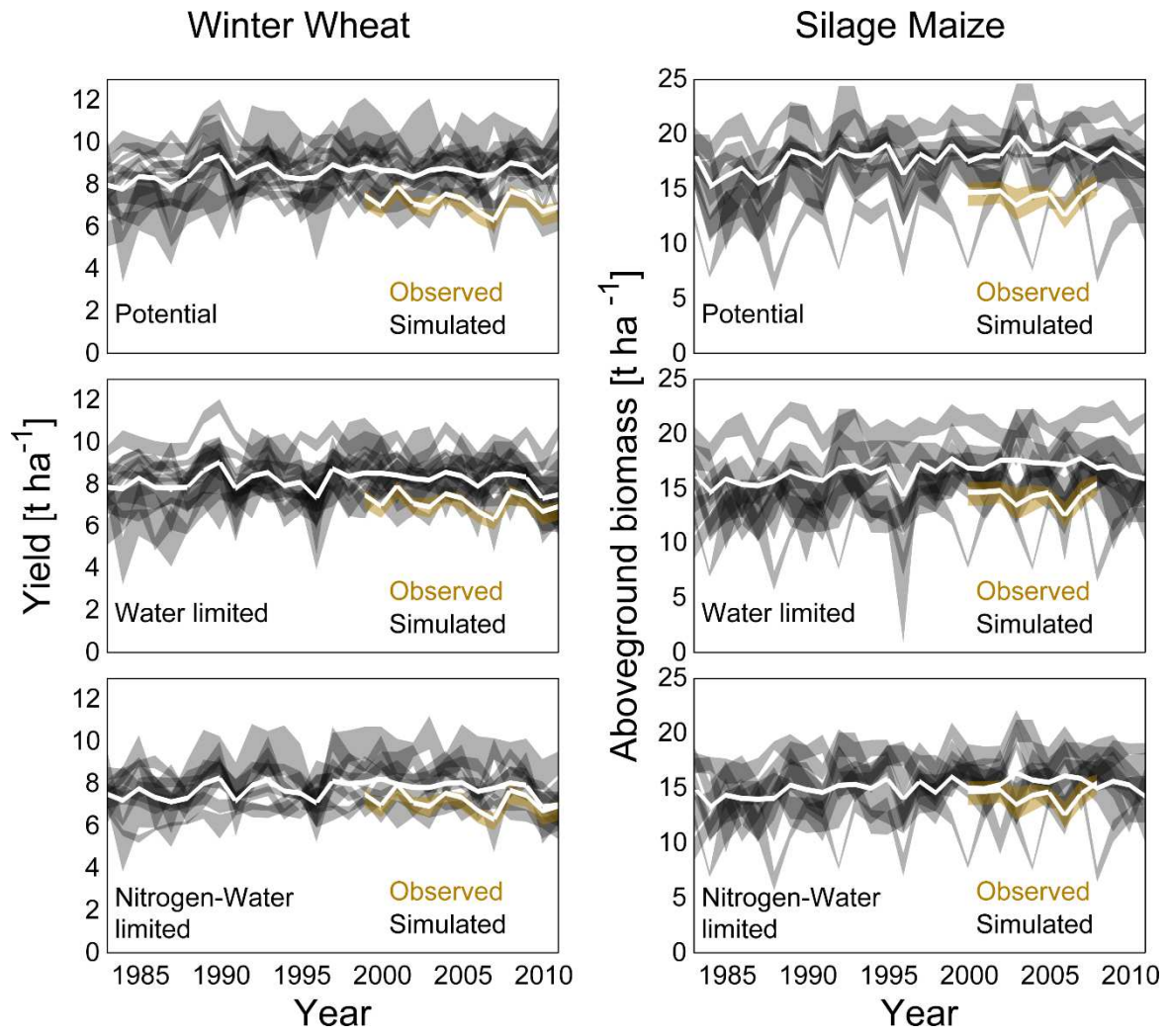
941

942 Fig. 4

943

944

945



946

947 Fig. 5

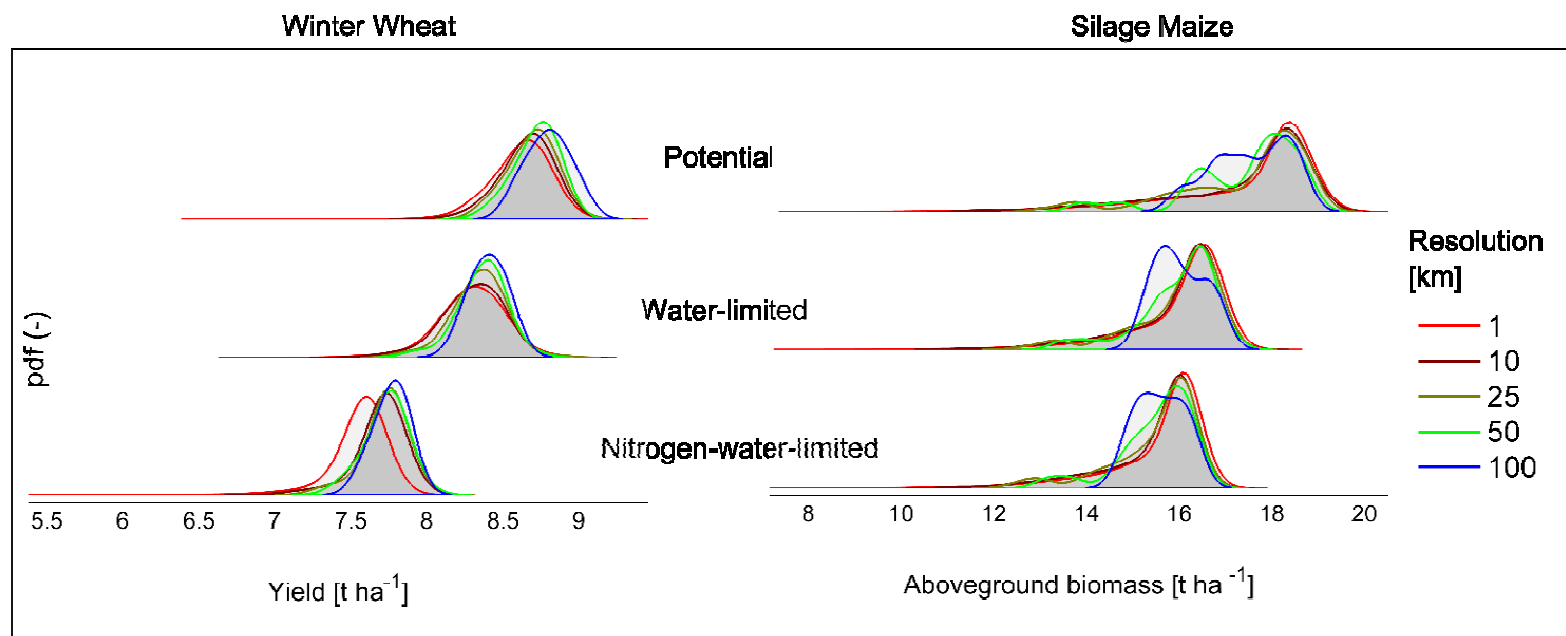
948

949

950

951

952



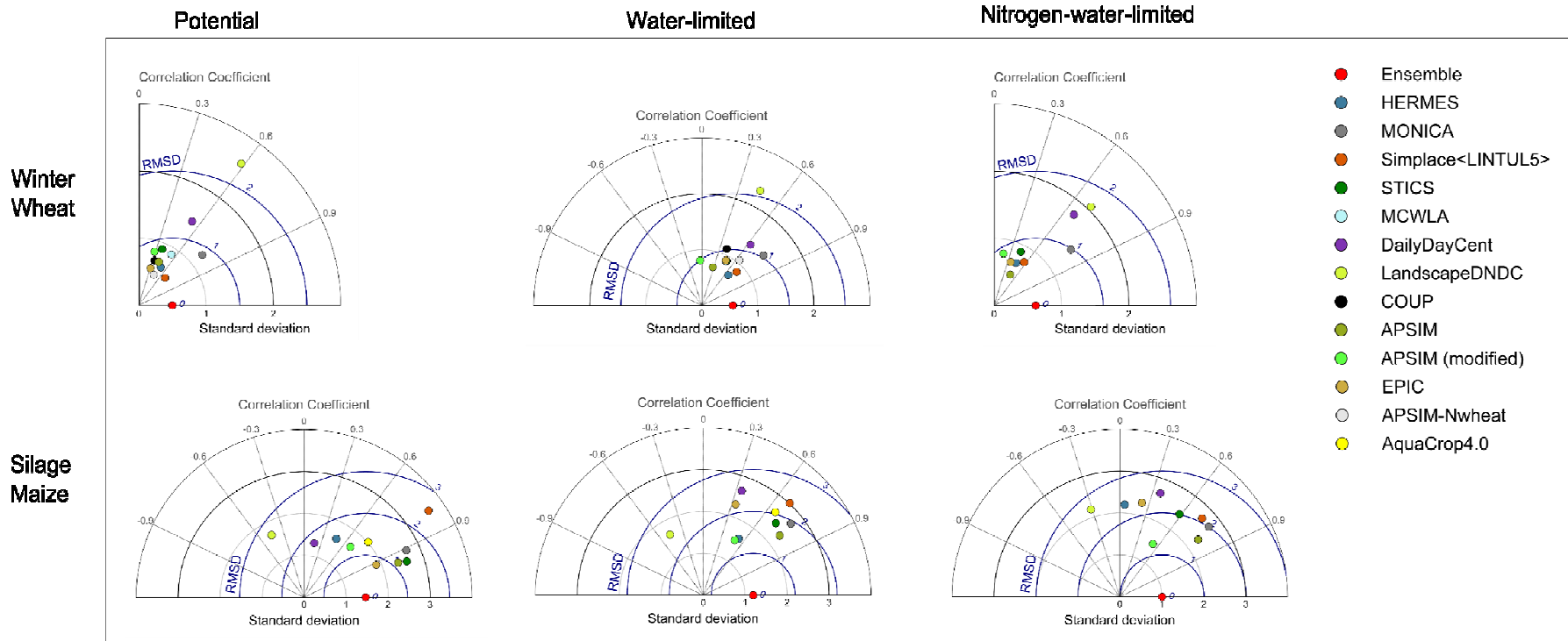
953

954 Fig. 6

955

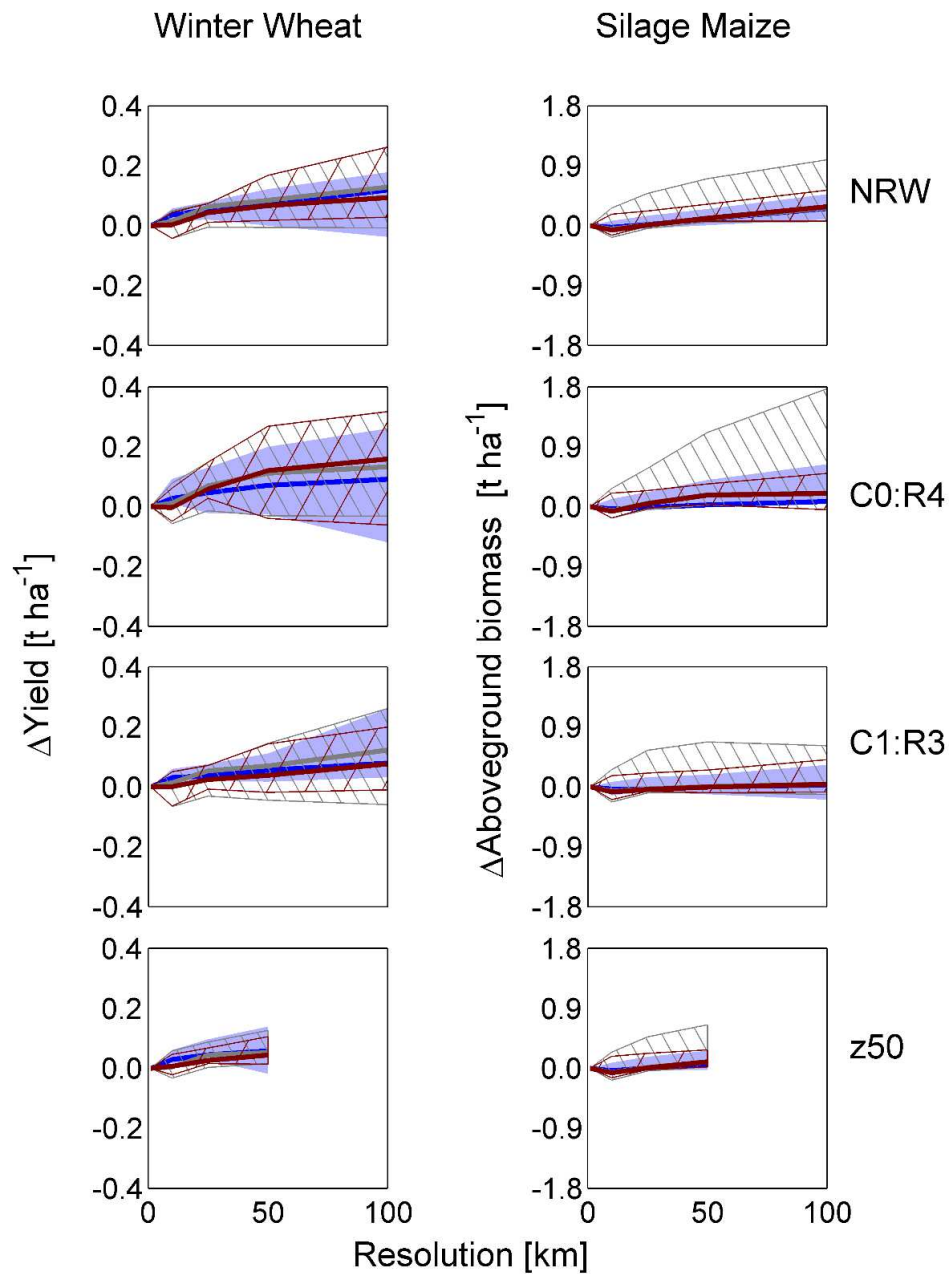
956

957



958

959 Fig. 7



960

961

962

963

Fig. 8